

Joint Channel Estimation and Signal Recovery for RIS-Empowered Multi-User Communications

Li Wei, Chongwen Huang, Qinghua Guo, *Senior Member, IEEE*, Zhaohui Yang, *Member, IEEE*, Zhaoyang Zhang, *Senior Member, IEEE*, George C. Alexandropoulos, *Senior Member, IEEE*,
Mérrouane Debbah, *Fellow, IEEE* and Chau Yuen, *Fellow, IEEE*

Abstract—Reconfigurable intelligent surfaces (RISs) have been recently considered as a promising candidate for energy-efficient solutions in future wireless networks. Their dynamic and low-power configuration enables coverage extension, massive connectivity, and low-latency communications. Due to a large number of unknown variables referring to the RIS unit elements and the transmitted signals, channel estimation and signal recovery in RIS-based systems are the ones of the most critical technical challenges. To address this problem, we focus on the RIS-assisted wireless communication system and present two joint channel estimation and signal recovery schemes based on message passing algorithms in this paper. Specifically, the proposed bidirectional scheme applies the Taylor series expansion and Gaussian approximation to simplify the sum-product procedure in the formulated problem. In addition, the inner iteration that adopts two variants of approximate message passing algorithms is incorporated to ensure robustness and convergence. Two ambiguities removal methods are also discussed in this paper. Our simulation results show that the proposed schemes show the superiority over the state-of-art benchmark method. We also provide insights on the impact of different RIS parameter settings on the proposed schemes.

Index Terms—Reconfigurable intelligent surfaces, message passing algorithms, channel estimation, signal recovery, Gaussian approximation.

I. INTRODUCTION

Reconfigurable intelligent surface (RIS) is a potential candidate technology for beyond fifth-generation (5G) wireless communications [1]–[6]. A large number of hardware-efficient passive reflecting elements are employed in a RIS to facilitate

L. Wei and C. Yuen are with the Engineering Product Development (EPD) Pillar, Singapore University of Technology and Design, Singapore 487372 (e-mails: wei_li@myemail.sutd.edu.sg, yuenchau@sutd.edu.sg).

C. Huang, Z. Yang and Z. Zhang are with the College of Information Science and Electronic Engineering, Zhejiang University, Hangzhou 310007, China, and Zhejiang Provincial Key Lab of Information Processing, Communication and Networking (IPCAN), Hangzhou 310007, China, and the International Joint Innovation Center, Zhejiang University, Haining 314400, China. C. Huang is also with Zhejiang-Singapore Innovation and AI Joint Research Lab, Hangzhou 310027, China. Z. Yang is also with the Zhejiang Laboratory, Hangzhou 31121, China. (e-mails: {chongwenhuang@zju.edu.cn, zhaohuiyang92@gmail.com, ning_ming@zju.edu.cn}).

Q. Guo is with the School of Electrical, Computer and Telecommunications Engineering, University of Wollongong, Wollongong, NSW 2522, Australia (e-mail: qguo@uow.edu.au).

G. C. Alexandropoulos is with the Department of Informatics and Telecommunications, National and Kapodistrian University of Athens, Panepistimiopolis Ilissia, 15784 Athens, Greece and also with the Technology Innovation Institute, Abu Dhabi, United Arab Emirates (e-mail: alexandg@di.uoa.gr).

M. Debbah is with the Technology Innovation Institute, 9639 Masdar City, Abu Dhabi, United Arab Emirates (email: merouane.debbah@tii.ae) and also with CentraleSupélec, University Paris-Saclay, 91192 Gif-sur-Yvette, France.

low-power, energy-efficient, high-speed, massive-connectivity, and low-latency communications [7]–[10]. Each unit element in a RIS can alter the phase of the incoming signal without requiring a dedicated power amplifier that is needed in conventional amplify-and-forward relaying systems [3], [10], [11]. As a result, RISs had gained much attention in recent years.

The energy efficiency potential of RIS in the scenario of outdoor multi-user multiple input single output communications was analyzed in [3], while [12] focused on an indoor scenario to illustrate the potential of RIS-based indoor positioning. It was shown in [13] and [14] that the potential of positioning is large even in the case of RISs with finite resolution unit elements and statistical channel knowledge. Recently, a novel passive beamforming and information transfer technique was proposed in [15] to enhance primary communications, as well as a two-step approach at the receiver to retrieve the information from both the transmitter and RIS. RIS-assisted communications in the millimeter-wave and terahertz bands were also lately investigated to deal with limited transmission distance problem [1]. Orthogonal and non-orthogonal multiple access in RIS-assisted communications were studied in [16] as cost-effective solutions for boosting spectrum/energy efficiency. The work in [17] proposed an RIS aided multi-user full-duplex two-way communication network to enhance user fairness, where RIS is effectively adjusted to mitigate the interference at the users with fully knowledge of channel information. The work in [18] focused on the RIS aided two-way device-to-device multi-pair OFDM communications and maximized the minimum bidirectional weighted sum-rate with perfect CSI. The existing research works have proved the great potential of RISs, however, most of the existing research works focusing on RIS configuration optimization were carried out with the assumption of the perfect channel state information. Thus, channel acquisition plays a significant role in RIS-assisted systems, and it is a challenging issue due to the incorporation of a large number of passive elements in RISs, specifically, the estimation of the cascaded channels, transmitter-to-RIS channel and RIS-to-receiver channel, brings many difficulties.

The recent works in [19] and [20] presented compressive sensing and deep learning approaches for recovering the involved channels and designing the RIS phase matrix. However, the deep learning approaches require extensive training during offline training phases, and the compressive sensing framework assumes that RIS has some active elements, i.e., a fully digital or hybrid analog and digital architecture is attached

at RIS. The architecture that has some active elements would increase the RIS hardware complexity and power consumption. A low-power radio frequency chain for channel estimation was considered in [5], which also requires additional energy consumption compared to passive RISs. Recently, the authors in [21] adopted PARAllel FACtor (PARAFAC) decomposition to estimate all involved channels with totally passive RIS elements, but the PARAFAC based methods require strict feasibility conditions with the excessively high complexity for a large number of RIS elements. In [22], the authors adopted a hierarchical training reflection design to progressively estimate channels over multiple time blocks, which has high complexity in the multiuser communication system. However, most of the existing works only consider the channel estimation part in RIS-assisted systems, while the joint channel estimation and signal recovery problem has not been well studied.

In [23], the authors adopted a two-stage approach to estimate channels and transmitted signal separately. Specifically, the cascaded channels are estimated using the PARAFAC method firstly, and then the signal is recovered based on the estimated channels. The existing literature applies similar methods, i.e., the channel information is obtained in the first stage, and then the signal is recovered in the second stage. Such a method cannot fully explore the characteristics of channels and transmitted signals due to separate channel estimation and signal recovery, and the training overhead is high in this two-stage method. Thus, some message passing algorithms based on factor graphs were proposed for joint estimation and signal recovery, such as bilinear generalized approximate message passing (BiGAMP) [24] and generalized sparse Bayesian learning algorithm [25]. In [26], the framework of expectation propagation was employed to perform joint channel estimation and decoding in massive multiple-input multiple-output (MIMO) systems with orthogonal frequency division multiplexing. In [27], the authors designed a Bayesian method for the effective channel estimation and signal recovery in grant-free non-orthogonal multiple access. In [28], the authors applied a new expectation maximization message passing algorithm combination for joint channel estimation and symbol detection. In [29], the authors proposed a multi-layer BiGAMP approach for handling the cascaded problem in amplify-and-forward relay communication systems, and the performance of joint channel estimation and signal detection in two-hop relay systems with one known channel was investigated. However, these approximate message passing (AMP) related algorithms are vulnerable to ill-conditioned measurement matrices that may cause divergence. Thus, some variants to improve this problem were proposed, such as damping method [30], bilinear adaptive generalized vector approximate message passing [31] and AMP with unitary transformation (UTAMP) [32], [33]. The above works in [30]–[33] provide some insights into the joint channel estimation and signal recovery in RIS-assisted communication systems, which motivates us to explore a new technique to reliably estimate channels and recover signal simultaneously with tolerable training overhead.

In this paper, we propose a novel joint channel estimation and signal detection algorithm in a RIS-assisted uplink wireless communication system, where a multi-antenna base

station (BS) serves multiple single-antenna users. Different from the existing methods, which estimate channels (with fixed number of pilots) and detect signal in two separate stages, we take advantage of iterative process to estimate channels and transmitted signal simultaneously, specifically, the estimated data in each iteration is used as virtual training signals to achieve better performance. Specifically, we formulate the joint channel estimation and signal recovery as an inference problem that estimates two cascaded channels and transmitted signal simultaneously. The factor graph and the related sum-product message passing rules of the formulated problem are developed, then we apply Taylor series expansion and Gaussian approximation to deal with the tricky inference problem. We also propose two schemes that improve the convergency by iteratively refining the estimates of the proposed algorithm. Moreover, to solve the issue of involved ambiguities in the formulated problem, two ambiguity removal approaches are investigated in this paper. The proposed algorithms are efficient and provide good channel estimation and signal recovery performance. Our extensive simulation results validate the effectiveness of the proposed techniques and their favorable performance. The main contributions of this paper are summarized as follows:

- 1) A proper system model of the joint channel estimation and signal detection in a RIS-assisted wireless system is established, and the factor representation is derived as well as the related message passing algorithms. Moreover, simplification of the message updating for efficient inference is studied in this work. Specifically, inspired by AMP derivations, we adopt Gaussian approximation and Taylor series expansion to derive a computationally efficient algorithm.
- 2) Based on the simplified algorithms, two efficient schemes that further improve the convergence are presented. One is bidirectional AMP (BAMP) and the other is bidirectional unitary transformation AMP (BUTAMP), for robustness and faster convergence. Specifically, all channels and transmitted signals can be recovered without divergence using the proposed two schemes.
- 3) We investigate the inherent ambiguities in the proposed algorithm, and two ambiguities removal methods are proposed. Specifically, the introduction of a large number of pilots could eliminate phase ambiguities and scaling ambiguities (the known parts in estimated channel and transmitted signal are termed as pilots), however, it is impractical to obtain these pilots directly, thus we investigate the efficient methods to obtain these pilots. In addition, the computational complexity is also analyzed. The proposed algorithms have the low computational complexity, which is dominated by matrix-vector multiplications.
- 4) We prove the effectiveness of the proposed algorithms through simulations and comparisons with some benchmark curves. It is shown that the proposed schemes can achieve favorable performance in various cases.

The remainder of this paper is organized as follows. In Section II, the system model is introduced. In Section III, the

factor graph and the proposed message passing algorithm are presented, we propose two schemes to further improve the convergence of the algorithms, and ambiguities removal and complexity analysis are also discussed. Section IV presents the numerical results of the proposed schemes. Finally, some conclusions are drawn in Section V.

Notation: Fonts a , \mathbf{a} , and \mathbf{A} represent scalars, vectors, and matrices, respectively. We use \mathbf{A}^T , \mathbf{A}^H , \mathbf{A}^{-1} and \mathbf{A}^\dagger to denote the transpose, Hermitian (conjugate transpose), inverse and pseudo-inverse of \mathbf{A} , respectively. The (m, n) -th entry of \mathbf{A} is denoted by a_{mn} . We use $|\cdot|$ and $(\cdot)^*$ to denote the modulus and conjugation, respectively. \propto denotes the proportional relationship between two quantities. Finally, notation $\text{diag}(\mathbf{a})$ represents a diagonal matrix with the entries of \mathbf{a} on its main diagonal.

II. SYSTEM MODEL

In this section, we first describe the system and signal models for the considered RIS-assisted wireless communication system, and then derive a message passing algorithm for the end-to-end wireless communication channel.

We consider the uplink communication between a BS equipped with K antenna elements and M single-antenna mobile users, as shown in the Fig. 1. We assume that this communication is realized via a discrete-element RIS deployed on the facade of a building in the vicinity of the BS side. The RIS is comprised of N unit cells of equal small size, and each made from metamaterials that are capable of adjusting their reflection coefficients. We assume that there is no direct signal path between the BS and the mobile users due to unfavorable propagation conditions, e.g., the presence of large obstacles. It should be noted that the existence of direct link has no impact on the proposed algorithms in this work, since direct link can be estimated with the off state of RIS elements using conventional methods.

The received discrete-time signals at BS from all M mobile users for T consecutive time slots can be compactly expressed with $\tilde{\mathbf{Y}} \in \mathbb{C}^{K \times T}$ given by

$$\tilde{\mathbf{Y}} \triangleq \tilde{\mathbf{H}}^r \Phi \tilde{\mathbf{H}}^b \tilde{\mathbf{X}} + \tilde{\mathbf{W}}, \quad (1)$$

where diagonal matrix Φ is the phase configuration for N RIS unit elements, which is full rank and usually chosen from low resolution discrete sets [13]; $\tilde{\mathbf{H}}^b \in \mathbb{C}^{N \times M}$ and $\tilde{\mathbf{H}}^r \in \mathbb{C}^{K \times N}$ denote the channel matrices between all users and RIS, and between RIS and BS, respectively; the matrix $\tilde{\mathbf{X}} \in \mathbb{C}^{M \times T}$ includes the M users transmitted signal within T time slots; and $\tilde{\mathbf{W}} \in \mathbb{C}^{K \times T}$ is the Additive White Gaussian Noise (AWGN) matrix with element having zero mean and variance N_0 .

In typical cellular configuration, the involved narrowband channels are correlated random vectors that are dependent of scattering geometry, however, for large number of antenna elements at RIS, the channels can be represented by sparse matrices in beam domain [34]–[38]. Thus, the n -th column in channel $\tilde{\mathbf{H}}^r$ is expressed as [39]

$$\tilde{\mathbf{H}}^r_{:,n} = \sum_{l=1}^{N_c} \alpha_{n,l} e^{-j2\pi d_{n,l}/\lambda_c} \mathbf{e}(\phi_{n,l}), \quad (2)$$

where N_c is the number of channel paths, $\alpha_{n,l} \sim \mathcal{CN}(0, 1)$ and $d_{n,l}, \phi_{n,l}$ are the channel attenuation, physical distance and AoD associated with the l -th path for the n -th element, respectively, λ_c denotes the signal wavelength, $\mathbf{e}(\phi_{n,l}) \in \mathbb{C}^{K \times 1}$ is the element array vector at the RIS side along with the direction of $\phi_{k,l}$, which satisfies $\|\mathbf{e}(\phi_{n,l})\|_2^2 = 1$ and can be given by

$$\mathbf{e}(\phi_{n,l}) = \frac{1}{\sqrt{K}} \left[1, e^{j\frac{2\pi d}{\lambda_c} \sin \phi_{n,l}}, \dots, e^{j\frac{2\pi d}{\lambda_c} (K-1) \sin \phi_{n,l}} \right]^T, \quad (3)$$

where d is the element spacing. Thus, the channel can be further represented by

$$\tilde{\mathbf{H}}^r = \mathbf{F}_1 \mathbf{H}^r \quad (4)$$

where \mathbf{H}^r is the angular domain channel, and \mathbf{F}_1 is $K \times K$ discrete Fourier transform (DFT) matrix, the q -th column of which is given by

$$[\mathbf{F}_1]_{:,q} = \frac{1}{\sqrt{K}} \left[1, e^{-j\frac{2\pi q}{K}}, \dots, e^{-j\frac{2\pi (K-1)q}{K}} \right]^T. \quad (5)$$

Thus, we have

$$\mathbf{H}^r = \mathbf{F}_1^H \tilde{\mathbf{H}}^r = \mathbf{F}_1^H \mathbf{E} \boldsymbol{\beta}, \quad (6)$$

where $\mathbf{E}_n = [\mathbf{e}(\phi_{n,1}), \mathbf{e}(\phi_{n,2}), \dots, \mathbf{e}(\phi_{n,N_c})] \in \mathbb{C}^{K \times N_c}$ and $\boldsymbol{\beta}_n = [\beta_{n,1}, \beta_{n,2}, \dots, \beta_{n,N_c}]^T \in \mathbb{C}^{N_c \times 1}$ with $\beta_{n,l} = \alpha_{n,l} e^{-j2\pi d_{n,l}/\lambda_c}$, and $\mathbf{E} \boldsymbol{\beta}$ is the collection of $\mathbf{E}_n \boldsymbol{\beta}_n$. Based on [39], the equivalent channel \mathbf{H}^r is sparse.

Similarly, the channel $\tilde{\mathbf{H}}^b$ can also be represented by sparse beam domain channel

$$\tilde{\mathbf{H}}^b = \mathbf{H}^b \mathbf{F}_2, \quad (7)$$

where the precoding matrix \mathbf{F}_2 is the $M \times M$ DFT matrix.

Thus, the input-output relationship (1) can be rewritten as

$$\tilde{\mathbf{Y}} \triangleq \mathbf{F}_1^H \mathbf{H}^r \Phi \mathbf{H}^b \mathbf{F}_2^H \tilde{\mathbf{X}} + \tilde{\mathbf{W}} \Rightarrow \mathbf{Y} \triangleq \mathbf{H}^r \Phi \mathbf{H}^b \mathbf{X} + \mathbf{W}, \quad (8)$$

where $\mathbf{Y} = \mathbf{F}_1 \tilde{\mathbf{Y}}$, $\mathbf{X} = \mathbf{F}_2^H \tilde{\mathbf{X}}$ and $\mathbf{W} = \mathbf{F}_1 \tilde{\mathbf{W}}$. Therefore, the beam domain representation yields an equivalent sparse channel estimation in beamspace. Generally, we can obtain the locally optimal performance or approximately optimal performance in separate channel estimation or signal recovery at the price of heavy training and computing. To cascade these locally optimal channel estimation and signal recovery together, the cascaded result usually is not the optimal performance for the whole communication system. To address this problem, we initially implement the joint channel estimation and signal recovery scheme without consuming too much computational complexity. Specifically, our objective is to jointly estimate the channel \mathbf{H}^r and \mathbf{H}^b , and transmitted signal \mathbf{X} during the signal transmission phase, which is provided in the following section.

III. PROBLEM FORMULATION AND MESSAGE PASSING ALGORITHM

A. Problem Formulation and Factor Graph Representation

The focus of this paper is to design an efficient receiver to estimate transmitted signal \mathbf{X} and all involved channels \mathbf{H}^b and \mathbf{H}^r . To this end, we formulate a two-layer estimation problem, and the framework is shown in Fig. 2. In the first layer, the input is transmitted signal \mathbf{X} , and the output is $\mathbf{U} = \mathbf{H}^b \mathbf{X}$. In the second layer, the input is \mathbf{U} , and the output is

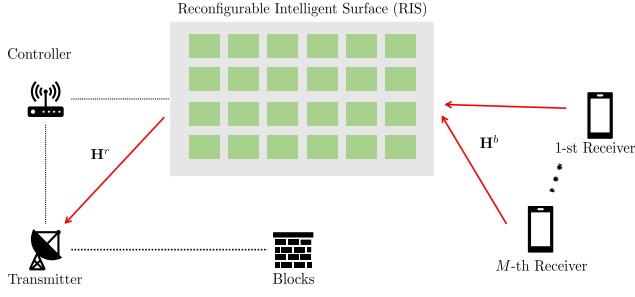


Figure 1. An uplink RIS-based wireless communication system consisting of a K -antenna BS and M single-antenna mobile users.

$\mathbf{A} = \mathbf{Q}\mathbf{U}$, with $\mathbf{Q} = \mathbf{H}^r \Phi$ that incorporates the unknown channel \mathbf{H}^r , and Φ is assumed to be known. The output \mathbf{A} is corrupted by the noise \mathbf{W} , which is interpreted as $\mathbf{Y} = \mathbf{A} + \mathbf{W}$.

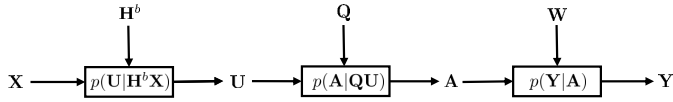


Figure 2. The framework of the formulated problem.

Thus, the joint probability $p(\mathbf{Q}, \mathbf{H}^b, \mathbf{X}, \mathbf{Y})$ can be factorized into

$$p(\mathbf{Q}, \mathbf{H}^b, \mathbf{X}, \mathbf{Y}) \propto p(\mathbf{X}) p(\mathbf{H}^b) p(\mathbf{U} | \mathbf{H}^b \mathbf{X}) p(\mathbf{Q}) p(\mathbf{A} | \mathbf{Q}\mathbf{U}) p(\mathbf{Y} | \mathbf{A}). \quad (9)$$

The probabilistic structure characterized by (9) is illustrated by Fig. 3. The circles represent variables and the squares represent factors. The purple circles denote the variable h_{nm}^b ; the red circles are variables x_{mt} ; and the blue circles represent q_{kn} . $p(x_{mt})$, $p(h_{nm}^b)$ and $p(q_{kn})$ are Gaussian priors of variables x_{mt} , h_{nm}^b and q_{kn} , respectively. f_{unt} is the (n, t) -th entry of $p(\mathbf{U} | \mathbf{H}^b \mathbf{X})$; f_{akt} is the (k, t) -th entry of $p(\mathbf{A} | \mathbf{Q}\mathbf{U})$; and f_{ykt} is the (k, t) -th element of $p(\mathbf{Y} | \mathbf{A})$. As shown in Fig. 3, the message updates bidirectionally, where the message flows from the left to right is termed as forward iteration, and the message flows conversely is backward iteration. The definitions of involved messages are summarized in Table. I, and according to the sum-product message passing rules, message updates in each layer are presented as follows:

1) *The First Layer*: The message from f_{unt} to x_{mt} in the ℓ -th iteration is given by

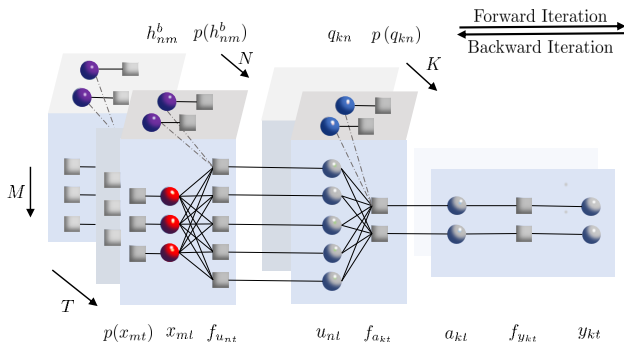


Figure 3. The factor graph of the joint channel estimation and signal recovery in RIS-empowered wireless communication systems.

Table I
MESSAGE DEFINITIONS IN THE FACTOR GRAPH.

The first layer			
$\mu_{x_{mt} \leftarrow f_{unt}}$	message from f_{unt} to x_{mt}	$\mu_{x_{mt} \rightarrow f_{unt}}$	message from x_{mt} to f_{unt}
$\mu_{f_{unt} \leftarrow h_{nm}^b}$	message from h_{nm}^b to f_{unt}	$\mu_{f_{unt} \rightarrow h_{nm}^b}$	message from f_{unt} to h_{nm}^b
$\mu_{f_{unt} \leftarrow u_{nt}}$	message from u_{nt} to f_{unt}	$\mu_{f_{unt} \rightarrow u_{nt}}$	message from f_{unt} to u_{nt}
The second layer			
$\mu_{u_{nt} \leftarrow f_{akt}}$	message from f_{akt} to u_{nt}	$\mu_{u_{nt} \rightarrow f_{akt}}$	message from u_{nt} to f_{akt}
$\mu_{f_{akt} \rightarrow q_{kn}}$	message from f_{akt} to q_{kn}	$\mu_{f_{akt} \leftarrow q_{kn}}$	message from q_{kn} to f_{akt}
$\mu_{f_{akt} \rightarrow a_{kt}}$	message from f_{akt} to a_{kt}	$\mu_{f_{akt} \leftarrow a_{kt}}$	message from a_{kt} to f_{akt}
$\mu_{a_{kt} \rightarrow f_{ykt}}$	message from a_{kt} to f_{ykt}	$\mu_{f_{ykt} \rightarrow y_{kt}}$	message from f_{ykt} to y_{kt}
$\mu_{a_{kt} \leftarrow f_{ykt}}$	message from f_{ykt} to a_{kt}		

$$\begin{aligned} & \mu_{x_{mt} \leftarrow f_{unt}}^\ell(x_{mt}) \\ &= f_{unt}^\ell \mu_{f_{unt} \leftarrow u_{nt}}^\ell \prod_{m' \neq m}^M \mu_{x_{m't} \rightarrow f_{unt}}^\ell \prod_{m=1}^M \mu_{f_{unt} \leftarrow h_{nm}^b}^\ell. \end{aligned} \quad (10)$$

The message from x_{mt} to f_{unt} in the $(\ell + 1)$ -th iteration is

$$\mu_{x_{mt} \rightarrow f_{unt}}^{\ell+1}(x_{mt}) = p(x_{mt}) \prod_{n' \neq n}^N \mu_{x_{mt} \leftarrow f_{u_{n't}}}^\ell(x_{mt}). \quad (11)$$

The message from f_{unt} to h_{nm}^b in the ℓ -th iteration can be expressed as

$$\begin{aligned} & \mu_{f_{unt} \rightarrow h_{nm}^b}^\ell(h_{nm}^b) \\ &= f_{unt}^\ell \mu_{f_{unt} \leftarrow u_{nt}}^\ell \prod_{m' \neq m}^M \mu_{f_{unt} \leftarrow h_{nm'}^b}^\ell \prod_{m=1}^M \mu_{x_{mt} \rightarrow f_{unt}}^\ell. \end{aligned} \quad (12)$$

The message from h_{nm}^b to f_{unt} in the $(\ell + 1)$ -th iteration is

$$\mu_{f_{unt} \leftarrow h_{nm}^b}^{\ell+1}(h_{nm}^b) = p(h_{nm}^b) \prod_{t' \neq t}^T \mu_{f_{u_{n't'}} \rightarrow h_{nm}^b}^\ell(h_{nm}^b). \quad (13)$$

The message from u_{nt} to f_{unt} in the ℓ -th iteration is given by

$$\mu_{f_{unt} \leftarrow u_{nt}}^\ell(u_{nt}) = \prod_{k=1}^K \mu_{u_{nt} \leftarrow f_{akt}}^\ell. \quad (14)$$

The message from f_{unt} to u_{nt} in the ℓ -th iteration is

$$\mu_{f_{unt} \rightarrow u_{nt}}^\ell(u_{nt}) = f_{unt} \prod_{m=1}^M \mu_{x_{mt} \rightarrow f_{unt}}^\ell \prod_{m=1}^M \mu_{f_{unt} \leftarrow h_{nm}^b}^\ell. \quad (15)$$

2) *The Second Layer*: The message from f_{akt} to u_{nt} in the ℓ -th iteration is

$$\begin{aligned} & \mu_{u_{nt} \leftarrow f_{akt}}^\ell(u_{nt}) \\ &= f_{akt}^\ell \mu_{f_{akt} \leftarrow a_{kt}}^\ell \prod_{n' \neq n}^N \mu_{u_{n't} \rightarrow f_{akt}}^\ell \prod_{n=1}^N \mu_{f_{akt} \leftarrow q_{kn}}^\ell. \end{aligned} \quad (16)$$

The message from u_{nt} to f_{akt} in the ℓ -th iteration is

$$\mu_{u_{nt} \rightarrow f_{akt}}^{\ell+1}(u_{nt}) = \mu_{f_{unt} \rightarrow u_{nt}} \prod_{k' \neq k}^K \mu_{u_{nt} \leftarrow f_{z_{k't}}}^\ell(u_{nt}). \quad (17)$$

The message from f_{akt} to q_{kn} in the ℓ -th iteration is

$$\begin{aligned} & \mu_{f_{akt} \rightarrow q_{kn}}^\ell(q_{kn}) \\ &= f_{akt}^\ell \mu_{f_{akt} \leftarrow a_{kt}}^\ell \prod_{n' \neq n}^N \mu_{f_{akt} \leftarrow q_{kn'}}^\ell \prod_{n=1}^N \mu_{u_{nt} \rightarrow f_{akt}}^\ell. \end{aligned} \quad (18)$$

The message from q_{kn} to f_{akt} in the $(\ell + 1)$ -th iteration is

$$\mu_{f_{a_{kt}}^{\ell+1} \leftarrow q_{kn}}(q_{kn}) = p(q_{kn}) \prod_{t' \neq t}^T \mu_{f_{v_{kt'}}^{\ell} \rightarrow q_{kn}}(q_{kn}). \quad (19)$$

3) *The Output Layer:* The message from $f_{a_{kt}}$ to a_{kt} in the ℓ -th iteration is

$$\mu_{f_{a_{kt}}^{\ell} \rightarrow a_{kt}}(a_{kt}) = f_{a_{kt}} \prod_{n=1}^N \mu_{f_{a_{kt}}^{\ell} \leftarrow q_{kn}} \prod_{n=1}^N \mu_{u_{nt} \rightarrow f_{a_{kt}}}. \quad (20)$$

The message from a_{kt} to $f_{a_{kt}}$ in the ℓ -th iteration is

$$\mu_{f_{a_{kt}}^{\ell} \leftarrow a_{kt}}(a_{kt}) = \mu_{a_{kt} \leftarrow f_{y_{kt}}}^{\ell}(y_{kt}). \quad (21)$$

The message from a_{kt} to $f_{y_{kt}}$ is

$$\mu_{a_{kt} \rightarrow f_{y_{kt}}}^{\ell}(y_{kt}) = \mu_{f_{a_{kt}}^{\ell} \rightarrow a_{kt}}(a_{kt}), \quad (22)$$

and the message from $f_{y_{kt}}$ to y_{kt} equals to

$$\mu_{f_{y_{kt}} \rightarrow y_{kt}}(y_{kt}) = f_{y_{kt}} \mu_{a_{kt} \rightarrow f_{y_{kt}}}^{\ell}(a_{kt}). \quad (23)$$

The message from $f_{y_{kt}}$ to a_{kt} is

$$\mu_{a_{kt} \leftarrow f_{y_{kt}}}(a_{kt}) = f_{y_{kt}} \mu_{f_{y_{kt}} \leftarrow y_{kt}}^{\ell}(y_{kt}). \quad (24)$$

4) *Beliefs of Estimated Variables:* The beliefs (approximate a posteriori distributions) of x_{mt} , h_{nm}^b and q_{kn} are respectively given by

$$\mu_{x_{mt}}(x_{mt}) = p(x_{mt}) \prod_{n=1}^N \mu_{x_{mt} \leftarrow f_{u_{nt}}}(x_{mt}), \quad (25)$$

$$\mu_{h_{nm}^b}(h_{nm}^b) = p(h_{nm}^b) \prod_{t=1}^T \mu_{f_{u_{nt}} \rightarrow h_{nm}^b}(h_{nm}^b), \quad (26)$$

$$\mu_{q_{kn}}(q_{kn}) = p(q_{kn}) \prod_{t=1}^T \mu_{f_{a_{kt}} \rightarrow q_{kn}}(q_{kn}). \quad (27)$$

B. Derivation and Approximation of Message Passing

We have derived the sum product algorithm with the factor graph in Fig. 3, however, exact implementation is impractical due to the involvement of numerous loops and both discrete and continuous-valued variables. Thus, the Gaussian approximation and Taylor series expansion are applied to further simplify the messages of loopy belief propagation (LBP) for efficient inference. In this section, we derive the approximate message passing algorithms for joint channel estimation and signal recovery in Fig. 3. The detailed derivation of each message is provided in Appendix. Here, we give the simplified messages processed by Gaussian approximated and Taylor series expansion.

In the first layer, the message from factor nodes to variables can be simplified as

$$\mu_{x_{mt} \leftarrow f_{u_{nt}}}(x_{mt}) \sim \mathcal{N}\left(x_{mt} \mid \frac{\hat{h}_{nm}^b \tilde{s}_{nt} + \hat{x}_{mt} |\hat{h}_{nm}^b|^2 v_{nt}^s}{|\hat{h}_{nm}^b|^2 v_{nt}^s + v_{nm}^b v_{nt}^s - v_{nm}^b |\tilde{s}_{nt}|^2}, \frac{1}{|\hat{h}_{nm}^b|^2 v_{nt}^s + v_{nm}^b v_{nt}^s - v_{nm}^b |\tilde{s}_{nt}|^2}\right), \quad (28)$$

$$\mu_{f_{u_{nt}} \rightarrow h_{nm}^b}(h_{nm}^b) \sim \mathcal{N}\left(h_{nm}^b \mid \frac{\hat{x}_{mt} \tilde{s}_{nt} + \hat{h}_{nm}^b |\hat{x}_{mt}|^2 v_{nt}^s}{|\hat{x}_{mt}|^2 v_{nt}^s + v_{mt}^x v_{nt}^s - v_{mt}^x |\tilde{s}_{nt}|^2}, \frac{1}{|\hat{x}_{mt}|^2 v_{nt}^s + v_{mt}^x v_{nt}^s - v_{mt}^x |\tilde{s}_{nt}|^2}\right).$$

The beliefs of two variables x_{mt} and h_{nm}^b are given as

$$\begin{aligned} \mu_{x_{mt}}(x_{mt}) &\sim \mathcal{N}(x_{mt} \mid \hat{x}_{mt}, v_{mt}^x), \\ \mu_{h_{nm}^b}(h_{nm}^b) &\sim \mathcal{N}(h_{nm}^b \mid \hat{h}_{nm}^b, v_{nm}^b). \end{aligned} \quad (29)$$

In the second layer, the message from factor nodes to variables can be simplified as

$$\begin{aligned} \mu_{u_{nt} \leftarrow f_{v_{kt}}}(u_{nt}) &\sim \mathcal{N}\left(u_{nt} \mid \frac{\hat{q}_{kn} \tilde{s}_{kt} + \hat{u}_{nt} |\hat{q}_{kn}|^2 v_{kt}^s}{|\hat{q}_{kn}|^2 v_{kt}^s + v_{kn}^q v_{kt}^s - v_{kn}^q |\tilde{s}_{kt}|^2}, \frac{1}{|\hat{q}_{kn}|^2 v_{kt}^s + v_{kn}^q v_{kt}^s - v_{kn}^q |\tilde{s}_{kt}|^2}\right), \\ \mu_{f_{a_{kt}} \rightarrow q_{kn}}(q_{kn}) &\sim \mathcal{N}\left(q_{kn} \mid \frac{\hat{u}_{nt} \tilde{s}_{kt} + \hat{q}_{kn} |\hat{u}_{nt}|^2 v_{kt}^s}{|\hat{u}_{nt}|^2 v_{kt}^s + v_{nt}^u v_{kt}^s - v_{nt}^u |\tilde{s}_{kt}|^2}, \frac{1}{|\hat{u}_{nt}|^2 v_{kt}^s + v_{nt}^u v_{kt}^s - v_{nt}^u |\tilde{s}_{kt}|^2}\right). \end{aligned} \quad (30)$$

The belief of variable q_{kn} is

$$\mu_{q_{kn}}(q_{kn}) \sim \mathcal{N}(q_{kn} \mid \hat{q}_{kn}, v_{kn}^q). \quad (31)$$

C. Two Proposed Schemes

The proposed bidirectional channel estimation and signal recovery problem is given by the factor graph Fig. 3, which is mainly composed of backward part and forward part. The backward part firstly estimates the intermediate variables of matrix \mathbf{Q} and matrix \mathbf{U} with the aid of received signals in the second layer, then the intermediate variables of signal \mathbf{X} and \mathbf{H}^b are estimated in the first layer, as shown in Alg. 1. In the forward part, the signal \mathbf{X} and \mathbf{H}^b are estimated in the first layer, then the unknown matrix \mathbf{Q} is estimated in the second layer, as shown in Alg. 2. The overall algorithm is shown in Alg. 1 and Alg. 2. The parameter ϵ is the threshold in the stop criterion, and it is selected as a small number, which is normally less than or equal to 10^{-4} . To further improve the estimation performance, we adopt an inner iteration in the estimation of matrix \mathbf{Q} , which leads to two schemes, BAMP algorithm and BUTAMP two-layer algorithm.

1) *BAMP Two-layer Algorithm:* We propose a BAMP algorithm to refine the estimation of matrix \mathbf{Q} , which improves the convergence of the whole algorithm. Specifically, the pilots $\mathbf{X}^p \in \mathbb{R}^{M \times T_p}$ are used in the initial iteration, and estimates of \mathbf{X} and \mathbf{H}^b are obtained in the first layer, then, the output $\hat{\mathbf{U}} = \hat{\mathbf{H}}^b \hat{\mathbf{X}}$ is considered as input of the estimation of \mathbf{Q} . Inspired by the GAMP algorithm, the obtained \mathbf{Q} is applied in subsequent iterations. Although the BAMP two-layer algorithm can estimate all involved unknown channels and signal simultaneously, the divergency issue still exists. This arises from the ill-conditioned matrix \mathbf{U} , which is the product of two Gaussian distributed matrices \mathbf{X} and \mathbf{H}^b . To improve the convergence, a damping factor β is introduced to the intermediate variables v^s in step 5 and 13 of Alg. 1 and V in step 7 and 15 in Alg. 2, i.e., $v^s(\ell) = (1 - \beta)v^s(\ell-1) + \beta v^s(\ell)$ and $V(\ell) = (1 - \beta)V(\ell-1) + \beta V(\ell)$.

2) *BUTAMP Two-layer Algorithm:* BAMP is sensitive to the damping factor, thus, to further improve the convergence, the BUTAMP is proposed for strong robustness. Specifically, the estimates \mathbf{X} and \mathbf{H}^b are obtained in the first layer with the

aid of pilots, then, the singular value decomposition (SVD) is performed for the estimate $\mathbf{U} = \mathbf{U}\mathbf{\Lambda}\mathbf{V}$. Thus, a new input-output relationship can be given as

$$\begin{aligned} \mathbf{Y} &= \mathbf{Q}\mathbf{U} + \mathbf{W} \Rightarrow \mathbf{Y}\mathbf{V}^H = \mathbf{Q}\mathbf{U}\mathbf{\Lambda} + \mathbf{W}\mathbf{V}^H \\ &\Rightarrow \mathbf{R} = \mathbf{Q}\tilde{\mathbf{U}} + \tilde{\mathbf{W}}, \end{aligned} \quad (32)$$

where $\tilde{\mathbf{U}} = \mathbf{U}\mathbf{\Lambda}$ is the transformed measurement matrix and $\mathbf{R} = \mathbf{Y}\mathbf{V}^H$ is the transformed received signal. Then, the estimate of \mathbf{Q} can be obtained from (32) using AMP with unitary transformation [32] with low computational cost.

Algorithm 1 Joint CE and Signal Detection Algorithm (1): Backward Iteration

Input: The received signal y_{kt} , and the number of maximum algorithmic iterations L . **Initialization:** Initialize $x_{mt} = 0$, $v_{mt}^x = 1$, $h_{nm}^b = 0$, $v_{nm}^b = 1$, $a_{kt} = 0$, and $v_{kt}^a = 1$.

- 1: **for** $\ell = 1, 2, \dots, L$ **do**
- 2: $\tilde{v}_{kt}^{(2)} = \left(\frac{1}{V_{kt}^{(2)}} + \frac{1}{v^w} \right)^{-1}$
- 3: $\tilde{z}_{kt}^{(2)} = \tilde{v}_{kt}^{(2)} \left(\frac{Z_{kt}^{(2)}}{V_{kt}^{(2)}} + \frac{y_{kt}}{v^w} \right)$
- 4: $\tilde{s}_{kt}^{(2)} = \frac{\tilde{z}_{kt}^{(2)} - Z_{kt}^{(2)}}{V_{kt}^{(2)}}$
- 5: $v_{kt}^s(2) = -\frac{\tilde{v}_{kt}^{(2)} - V_{kt}^{(2)}}{V_{kt}^{(2)^2}}$
- 6: $\Sigma_{nt}^u = \left(\sum_{k=1}^K |\hat{q}_{kn}|^2 v_{kt}^s(2) \right)^{-1}$
- 7: $R_{nt}^u = \hat{u}_{nt} \left(1 + \Sigma_{nt}^u \sum_{k=1}^K v_{kn}^q |\tilde{s}_{kt}^{(2)}|^2 - v_{kn}^q v_{kt}^s(2) \right) + \Sigma_{nt}^u \sum_{k=1}^K \hat{q}_{kn} \tilde{s}_{kt}^{(2)}$
- 8: $\Sigma_{kn}^q = \left(\sum_{t=1}^T |\hat{u}_{nt}|^2 v_{kt}^s(2) \right)^{-1}$
- 9: $R_{kn}^q = \hat{q}_{kn} \left(1 + \Sigma_{kn}^q \sum_{t=1}^T v_{nt}^u |\tilde{s}_{kt}^{(2)}|^2 - v_{nt}^u v_{kt}^s(2) \right) + \Sigma_{kn}^q \sum_{t=1}^T \hat{u}_{nt} \tilde{s}_{kt}^{(2)}$
- % Message passing in the first layer
- 10: $\tilde{v}_{nt}^{(1)} = \left(\frac{1}{V_{nt}^{(1)}} + \frac{1}{\Sigma_{nt}^u} \right)^{-1}$
- 11: $\tilde{z}_{nt}^{(1)} = \tilde{v}_{nt}^{(1)} \left(\frac{Z_{nt}^{(1)}}{V_{nt}^{(1)}} + \frac{R_{nt}^u}{\Sigma_{nt}^u} \right)$
- 12: $\tilde{s}_{nt}^{(1)} = \frac{\tilde{z}_{nt}^{(1)} - Z_{nt}^{(1)}}{V_{nt}^{(1)}}$
- 13: $v_{nt}^s(1) = -\frac{\tilde{v}_{nt}^{(1)} - V_{nt}^{(1)}}{V_{nt}^{(1)^2}}$
- 14: $\Sigma_{mt}^x = \left(\sum_{n=1}^N |\hat{h}_{nm}^b|^2 v_{nt}^s(1) \right)^{-1}$
- 15: $R_{mt}^x = \hat{x}_{mt} \left(1 - \Sigma_{mt}^x \sum_{n=1}^N v_{nm}^b v_{nt}^s(1) \right) + \Sigma_{mt}^x \sum_{n=1}^N \hat{h}_{nm}^b \tilde{s}_{nt}^{(1)}$
- 16: $\Sigma_{nm}^b = \left(\sum_{t=1}^T |\hat{x}_{mt}|^2 v_{nt}^s(1) \right)^{-1}$
- 17: $R_{nm}^b = \hat{b}_{nm} \left(1 + \Sigma_{nm}^b \sum_{t=1}^T v_{mt}^x |\tilde{s}_{nt}^{(1)}|^2 - v_{mt}^x v_{nt}^s(1) \right) + \Sigma_{nm}^b \sum_{t=1}^T \hat{x}_{mt} \tilde{s}_{nt}^{(1)}$

3) *Ambiguities Removal:* Given the estimates $(\hat{\mathbf{H}}^r, \hat{\mathbf{H}}^b, \hat{\mathbf{X}})$ that the proposed algorithm returns for $(\mathbf{H}^r, \mathbf{H}^b, \mathbf{X})$, the following mean squared errors quantify how close the estimates are from the real values:

$$\begin{aligned} \text{MSE}_r &= \frac{\|\mathbf{H}^r - \hat{\mathbf{H}}^r\|_F^2}{KN}, & \text{MSE}_b &= \frac{\|\mathbf{H}^b - \hat{\mathbf{H}}^b\|_F^2}{NM}, \\ \text{MSE}_x &= \frac{\|\mathbf{X} - \hat{\mathbf{X}}\|_F^2}{MT}. \end{aligned} \quad (33)$$

Algorithm 2 Joint CE and Signal Detection Algorithm (2): Forward Iteration

- 1: $v_{mt}^x = \left(\frac{1}{\Sigma_{mt}^x} + \frac{1}{v_0^x} \right)^{-1}$
 - 2: $\hat{x}_{mt} = v_{mt}^x \left(\frac{R_{mt}^x}{\Sigma_{mt}^x} + \frac{\hat{x}_0^x}{v_0^x} \right)$
 - 3: $v_{nm}^b = \left(\frac{1}{\Sigma_{nm}^b} + \frac{1}{v_0^b} \right)^{-1}$
 - 4: $\hat{h}_{nm}^b = v_{nm}^b \left(\frac{R_{nm}^b}{\Sigma_{nm}^b} + \frac{\hat{h}_0^b}{v_0^b} \right)$
 - 5: $\bar{V}_{nt}^{(1),\ell+1} = \sum_{m=1}^M |\hat{x}_{mt}^{\ell+1}|^2 v_{nm}^{b,\ell+1} + |\hat{h}_{nm}^{b,\ell+1}|^2 v_{mt}^{x,\ell+1}$
 - 6: $\bar{Z}_{nt}^{(1),\ell+1} = \sum_{m=1}^M \hat{x}_{mt}^{\ell+1} \hat{h}_{nm}^{b,\ell+1}$
 - 7: $V_{nt}^{(1),\ell+1} = \bar{V}_{nt}^{(1),\ell+1} + \sum_{m=1}^M v_{mt}^{x,\ell+1} v_{nm}^{b,\ell+1}$
 - 8: $Z_{nt}^{(1),\ell+1} = \bar{Z}_{nt}^{(1),\ell+1} - \tilde{s}_{nt}^{(1)} \bar{V}_{nt}^{(1),\ell+1}$
 - 9: $v_{nt}^u = \left(\frac{1}{\Sigma_{nt}^u} + \frac{1}{v_{u,nt}^0} \right)^{-1}$
 - 10: $\hat{u}_{nt} = v_{nt}^u \left(\frac{R_{nt}^u}{\Sigma_{nt}^u} + \frac{\hat{u}_0^u}{v_{u,nt}^0} \right)$
 - 11: $v_{kn}^q = \left(\frac{1}{\Sigma_{kn}^q} + \frac{1}{v_0^q} \right)^{-1}$
 - 12: $\hat{q}_{kn} = v_{kn}^q \left(\frac{R_{kn}^q}{\Sigma_{kn}^q} + \frac{\hat{q}_0^q}{v_0^q} \right)$
 - 13: $\bar{V}_{kt}^{(2),\ell+1} = \sum_{n=1}^N |\hat{u}_{nt}^{\ell+1}|^2 v_{kn}^{q,\ell+1} + |\hat{q}_{kn}^{(2),\ell+1}|^2 v_{nt}^{u,\ell+1}$
 - 14: $\bar{Z}_{kt}^{(2),\ell+1} = \sum_{n=1}^N \hat{u}_{nt} \hat{q}_{kn}^{\ell+1}$
 - 15: $V_{kt}^{(2),\ell+1} = \bar{V}_{kt}^{(2),\ell+1} + \sum_{n=1}^N v_{nt}^{u,\ell+1} v_{kn}^{q,\ell+1}$
 - 16: $Z_{kt}^{(2),\ell+1} = \bar{Z}_{kt}^{(2),\ell+1} - \tilde{s}_{kt}^{(2)} \bar{V}_{kt}^{(2),\ell+1}$
 - 17: **Until** $\frac{\|\hat{\mathbf{H}}^{b,\ell} \hat{\mathbf{X}}^\ell - \hat{\mathbf{H}}^{b,\ell-1} \hat{\mathbf{X}}^{\ell-1}\|_F^2}{\|\hat{\mathbf{H}}^{b,\ell} \hat{\mathbf{X}}^\ell\|_F^2} \leq \epsilon$ or $\ell = L$
 - 18: **end for**
- Output:** $\hat{\mathbf{H}}^{b,\ell}$, $\hat{\mathbf{Q}}^\ell$ and $\hat{\mathbf{X}}^\ell$.
-

Note that in matrix factorization, there is an inherent ambiguity in recovering the couple $(\mathbf{H}^b, \mathbf{X})$ and (\mathbf{Q}, \mathbf{U}) . As a matter of fact, for any invertible unitary matrix $\mathbf{C}_1 \in \mathcal{R}^{M \times M}$ and $\mathbf{C}_2 \in \mathcal{R}^{M \times M}$, the couples $(\mathbf{H}^b \mathbf{C}_1, \mathbf{C}_1^{-1} \mathbf{X})$ and $(\mathbf{Q} \mathbf{C}_2, \mathbf{C}_2^{-1} \mathbf{U})$ generates the same values as $(\mathbf{H}^b, \mathbf{X})$ and (\mathbf{Q}, \mathbf{U}) . The existence of ambiguities undermines the estimation performance of the proposed algorithms, thus, it is necessary to remove or mitigate the inherent ambiguities. Moreover, due to the existence of three unknown matrices, the ambiguity issue in the proposed scheme is much more complex than that in the single layer bilinear case, such as BiG-AMP.

Inspired by the nonnegative matrix factorization in [40], we present an empirical parameter setting for the identifiability of the proposed algorithms. The proposed schemes have a high probability to give essentially unique estimates if the zero entries of \mathbf{H}^r has the density (number of nonzero entries over the number of entries) less than $(1 - \frac{N}{K})$ [40]. Moreover, it should be noted that the sparser \mathbf{H}^b , \mathbf{H}^r and \mathbf{X} they are, the lower Cramér–Rao lower bound on the accuracy of the estimates it is [40].

In order to eliminate scaling ambiguities, the first K_p rows of matrix \mathbf{H}^r are assumed to be known [41]. In addition, to remove the phase ambiguity, we adopt the method in [42]. In particular, the transmitted signal is designed to be a full-rank matrix. However, the cost is unreasonably high to obtain the knowledge of K_p rows in channel matrix \mathbf{H}^r in a large system. Thus, a lower cost ambiguities removal method is proposed.

Specifically, the portion in channel \mathbf{H}^r can be obtained

using bilinear recovery methods with the aid of pilot part in transmitted signals. Specifically,

$$\mathbf{Y}_p \triangleq \mathbf{H}_p^r \Phi \mathbf{H}^b \mathbf{X}_p + \mathbf{W}_p, \quad (34)$$

where $\mathbf{H}_p^r \in \mathbb{C}^{K_p \times N}$ and $\mathbf{X}_p \in \mathbb{C}^{M \times T_p}$ are the portion of channel \mathbf{H}^r and transmitted signal \mathbf{X} , respectively. $\mathbf{Y}_p \in \mathbb{C}^{K_p \times T_p}$ and $\mathbf{W}_p \in \mathbb{C}^{K_p \times T_p}$ are the portion in the received signal \mathbf{Y} and noise \mathbf{W} , respectively. Based on the pilot part, the portion of channel can be estimated using PARAFAC decomposition method or BiG-AMP method.

PARAFAC method leverages multiple phase matrices Φ to decompose the high-dimensional received signals, and it can recover the involved channels through a linear combination of multiple rank-one tensors (the details are referred to our previous work [21]). In addition, BiG-AMP is a generalized bilinear matrix recovery method, it estimates the involved channels simultaneously [24]. The obtained portion of \mathbf{H}^r can be further used in joint channel estimation and signal recovery, as shown in Alg. 1 and Alg. 2.

D. Complexity Analysis

The computational cost of the proposed BAMP algorithm is mainly dominated by componentwise squares of \mathbf{Q} , \mathbf{U} , \mathbf{H}^b and \mathbf{X} . Specifically, in the first layer, the computation complexity is dominated by the computation of \mathbf{H}^b and \mathbf{X} related componentwise squares in line 14~17 in Alg. 1 and line 5 in Alg. 2, which is $\mathcal{O}(NMT)$; and in the second layer, the complexity mainly arises from the computation of \mathbf{Q} and \mathbf{U} related componentwise squares in line 6~9 in Alg. 1 and line 13 in Alg. 2, which is $\mathcal{O}(KNT)$. Thus, the total computational cost of the proposed algorithm is $\mathcal{O}((KNT + NMT)L)$ with L being the iteration number.

IV. SIMULATION RESULTS

In this section, we present computer simulation results for the performance of the proposed two schemes. We have particularly simulated the NMSE using the metrics $\|\mathbf{H}^b - \hat{\mathbf{H}}^b\|^2 \|\mathbf{H}^b\|^{-2}$, $\|\mathbf{H}^r - \hat{\mathbf{H}}^r\|^2 \|\mathbf{H}^r\|^{-2}$ and $\|\mathbf{X} - \hat{\mathbf{X}}\|^2 \|\mathbf{X}\|^{-2}$. The scaling ambiguity of the proposed algorithms has been removed with the aid of the first K_p rows of the channel matrix \mathbf{H}^r . All normalized mean square error (NMSE) curves were obtained after averaging over 500 independent Monte Carlo channel realizations. The iteration stop criterion $\epsilon = 10^{-4}$. We compare the proposed methods with the state-of-art method, the BiGAMP+least squares (LS) method. Specifically, this method consists of two stages: the first stage estimates two channels \mathbf{H}^r and \mathbf{H}^b based on the pilot part $\mathbf{X}_p \in \mathbb{C}^{M \times T_p}$ using BiGAMP; then the data part $\mathbf{X}_d \in \mathbb{C}^{M \times (T-T_p)}$ is estimated based on the obtained channels using the LS in the second stage.

The NMSE performance comparison of the BUTAMP two layers algorithm and BAMP two layers algorithm versus the signal-to-noise ratio (SNR) is given in Fig. 4. The parameter settings are $M = 100$, $K = 500$, $T = 200$, $N = 200$ and $K_p = 150$, and the damping factor β in BAMP method is set 0.3. In the proposed algorithms, the pilot length is set $T_p = 100$. It can be observed from the figure that the

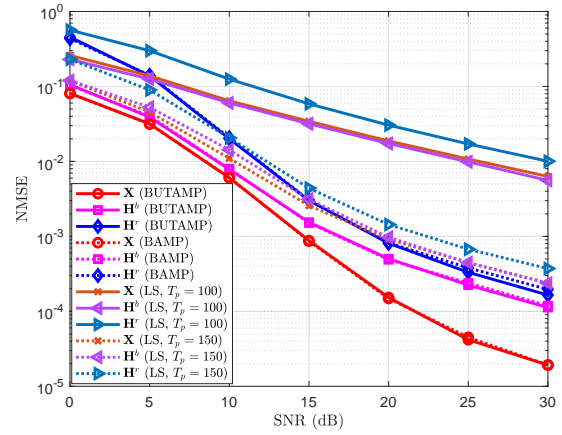


Figure 4. NMSE performance comparisons of the two proposed algorithms with baseline method (BiGAMP+LS) versus the SNR in dB for $M = 100$, $K = 500$, $T = 200$ and $N = 200$.

NMSE performance of the two proposed schemes is similar. In addition, the proposed algorithms consistently show great advantages compared with the benchmark. Specifically, there is about 18 dB gap between the proposed algorithms and the baseline method for the same pilot length $T_p = 100$. Even in the unfair setting ($T_p = 100$ for the proposed algorithms and $T_p = 150$ for the baseline method), there is about 4 dB gap between the proposed schemes and the benchmark in estimation of \mathbf{H}^b , and the gap in the estimation of \mathbf{X} is even larger. This behavior substantiates the favorable performance of our proposed schemes.

We evaluate the influence of pilot part in the Fig. 5 and Fig. 6. The minimum number of pilots T_p in \mathbf{X} required for the proposed algorithms is evaluated in Fig. 5 with $M = 100$, $K = 500$, $N = 100$, $T = 600$, and $T_p = 180, 200, 240$. It can be observed from the figure that the ratio $T_p/T = 0.3$ can achieve the similar performance with the case of higher ratio, which means the ratio of pilots in \mathbf{X} with 0.3 that is enough to achieve the best performance among all cases. In addition, we evaluate the impact of K_p in \mathbf{H}^r in Fig. 6 with $M = 100$, $K = 500$, $N = 100$, $T = 600$, and $K_p = 120, 150, 180$. As shown in figure, the larger K_p increases the whole performance. Taking the estimation of \mathbf{X} as an example, the gap between the case with $K_p = 120$ and that with $K_p = 150$ is about 9 dB, and the gap between the case with $K_p = 150$ and that with $K_p = 180$ reduces to 1.5 dB. The trend of estimations of \mathbf{H}^r and \mathbf{H}^b is similar, and the performance improvement is even larger than the estimation of \mathbf{X} , which substantiates that larger K_p could bring more benefit in the proposed algorithm.

The performance evaluation of the proposed BAMP two layers algorithm versus the SNR with various values of RIS elements $N = 150, 200$ and 300 is given in Fig. 7. The parameter settings are $M = 100$, $K = 500$, $T = 200$, $T_p = 100$ and $K_p = 150$, and the damping factor β is set 0.3. It is evident that there exists an increasing performance loss when N increases, and the gap becomes larger with the increase of SNR, e.g., the gap between the NMSE of \mathbf{X} with $N = 150$ and that with $N = 200$ is 5 dB, which is smaller than the gap between cases with $N = 150$ and that with $N = 300$.

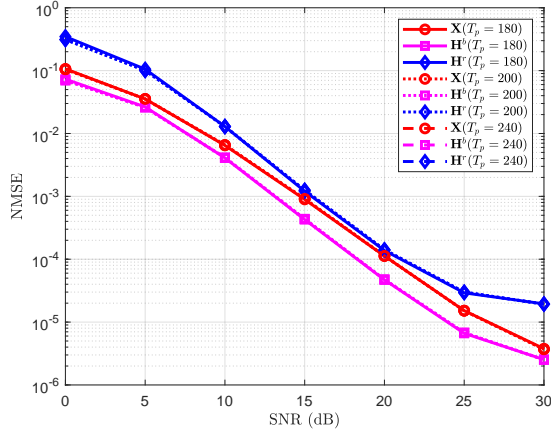


Figure 5. NMSE performance comparisons of the BAMP two layers algorithm versus the SNR in dB for $M = 100$, $K = 500$, $N = 100$, $T = 600$ and various values of T_p .

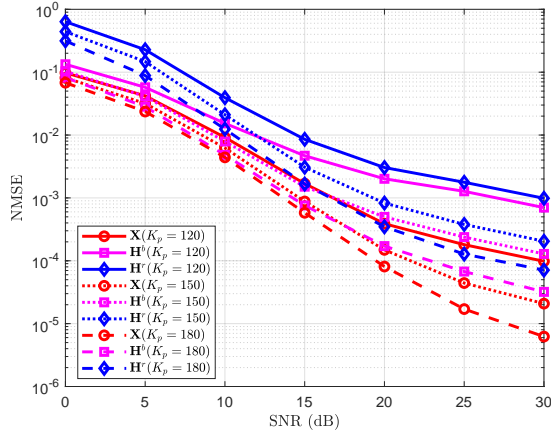


Figure 6. NMSE performance comparisons of the BAMP two layers algorithm versus the SNR in dB for $M = 100$, $K = 500$, $N = 200$, $T = 200$ and various values of K_p .

In those cases, the number of unknown variables for estimation increases, which results in performance loss.

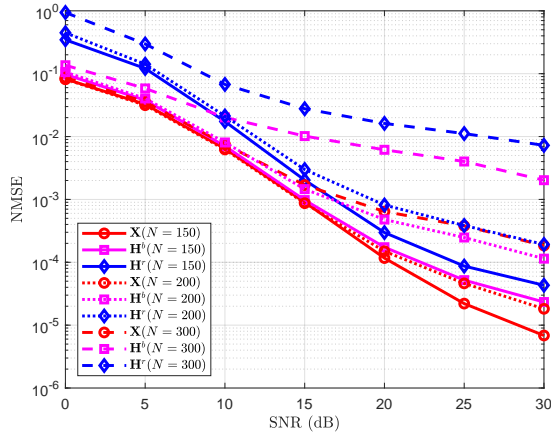


Figure 7. NMSE performance comparisons of the BAMP two layers algorithm versus the SNR in dB for $M = 100$, $K = 500$, $T = 200$ and various values of RIS elements N .

The performance evaluation of the BUTAMP two layers algorithm and BAMP two layers algorithm versus SNR with different damping factors are given in Fig. 8 and Fig. 9, respectively. The parameter settings are $M = 100$, $K = 500$,

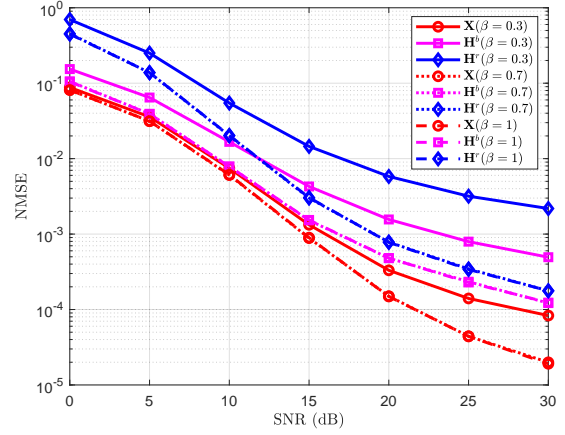


Figure 8. NMSE performance comparisons of the BUTAMP two layers algorithm versus the SNR in dB for $M = 100$, $K = 500$, $T = 200$, $N = 200$ and various values of damping factor.

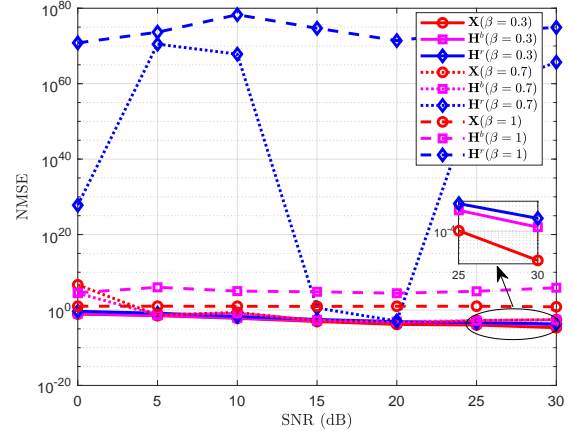


Figure 9. NMSE performance comparisons of the BAMP two layers algorithm versus the SNR in dB for $M = 100$, $K = 500$, $T = 200$, $N = 200$ and various values of damping factor.

$T = 200$, $N = 200$, $T_p = 100$ and $K_p = 150$. It can be observed from Fig. 8 that the BUTAMP two layers algorithm converges with different damping factors, however, the BAMP two layers algorithm diverges easily with inappropriate damping factors. Specifically, the BUTAMP two layers algorithm shows the similar NMSE performance for damping factors $\beta = 0.7$ and $\beta = 1$, and all cases converge with the increase of SNR, e.g., the gap of \mathbf{X} estimates between $\beta = 0.3$ and $\beta = 1$ is about 7 dB. Different from the Fig. 8, the NMSE performance of the BAMP two layers algorithm drastically decreases with changes of damping factor in Fig. 9. Specifically, the BAMP two layers algorithm diverges with $\beta = 0.7$ and $\beta = 1$. By comparing Fig. 8 and Fig. 9, we can see that the BUTAMP algorithm is more robust to damping factors.

The convergence of two proposed algorithms is presented in Fig. 10. The parameter setting is $M = 100$, $K = 500$, $N = 200$ and $T = 200$. It can be observed from the figure that both algorithms have less number of iterations with the increase of SNR, and BAMP algorithm requires more iterations to converge compared with BUTAMP algorithm, specifically, BAMP algorithm requires 28 iterations while BUTAMP only requires 18 iterations at SNR= 20 dB, which substantiates the

favorable convergence performance of BUTAMP algorithm.

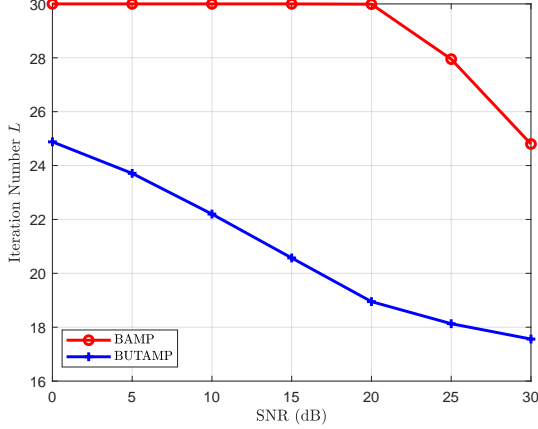


Figure 10. Number of iterations versus the SNR in dB for $M = 100$, $K = 500$, $N = 200$, $T = 200$ for the proposed BAMP and BUTAMP two layers algorithms.

V. CONCLUSION

In this paper, we proposed two message passing schemes for joint channel estimation and signal recovery in RIS-assisted wireless communication systems, which capitalizes on the factor graph and approximate message passing algorithms. All involved channels are estimated and the transmitted signal is recovered through bidirectional two-layer algorithms, BAMP algorithm and BUTAMP algorithm, at the lower computational cost and better convergence performance. Ambiguities removal methods and computational analysis are also presented in this paper. Our simulation results showed that the proposed two schemes have similar performance and BUTAMP algorithm is more robust to damping factors, and two proposed schemes showed superiority over the benchmark scheme. In addition, we observed that the pilot length and the number of RIS elements exert a significant effect on our proposed algorithm. Although the proposed algorithms are designed for multiple single-antenna users in uplink, they can be applied in uplink multi-antenna users and downlink single multi-antenna user case. In addition, with the proper design of distributed control networks to exchange information among different users, this work can be extended to downlink multiple multi-antenna users.

APPENDIX

The message passing between variables and factor nodes in two layers, and the simplification of intermediate variables are derived in this part.

1) *The First Layer (Approximated Factor-to-Variable Messages)*: We define the approximate posterior distribution of \mathbf{U}

$$\begin{aligned} \xi_{nt}^u &= p(u_{nt} | \mathbf{Y}) = x_{mt} \mu_{u_{nt} \leftarrow h_{nm}^b}(h_{nm}^b) \\ &+ \sum_{m' \neq m} \mu_{x_{m't} \rightarrow f_{u_{nt}}}(x_{m't}) \mu_{f_{u_{nt}} \leftarrow h_{nm'}^b}(h_{nm'}^b). \end{aligned} \quad (35)$$

Thus, the mean and variance of associate random variable ξ_{nt}^u are

$$\begin{aligned} \mathbb{E}[\xi_{nt}^u] &= x_{mt} \hat{h}_{nt \leftarrow nm}^b + \sum_{m' \neq m} \hat{h}_{nt \leftarrow nm'}^b \hat{x}_{m't \rightarrow nt} \\ &= x_{mt} \hat{h}_{nt \leftarrow nm}^b + Z_{nt \setminus m}, \end{aligned} \quad (36)$$

$$\begin{aligned} \text{Var}[\xi_{nt}^u] &= |x_{mt}|^2 v_{nt \leftarrow nm}^b + \sum_{m' \neq m} |\hat{x}_{m't \rightarrow nt}|^2 v_{nt \leftarrow nm'}^b \\ &+ |\hat{h}_{nt \leftarrow nm'}^b|^2 v_{m't \rightarrow nt}^x + v_{nt \leftarrow nm'}^b v_{m't \rightarrow nt}^x \\ &= |x_{mt}|^2 v_{nt \leftarrow nm}^b + V_{nt \setminus m}, \end{aligned} \quad (37)$$

where $\hat{h}_{nt \leftarrow nm}^b$ and $v_{nt \leftarrow nm}^b$ are the mean and variance of the message $\mu_{f_{u_{nt}} \leftarrow h_{nm}^b}$, respectively. $\hat{x}_{m't \rightarrow nt}$ and $v_{m't \rightarrow nt}^x$ are the mean and variance of the message $\mu_{x_{m't} \rightarrow f_{u_{nt}}}$.

We define

$$\begin{aligned} Z_{nt}^{(1)} &= \sum_{m=1}^M \hat{h}_{nt \leftarrow nm}^b \hat{x}_{m't \rightarrow nt}, \\ V_{nt}^{(1)} &= \sum_{m=1}^M |\hat{x}_{m't \rightarrow nt}|^2 v_{nt \leftarrow nm}^b + |\hat{h}_{nt \leftarrow nm}^b|^2 v_{m't \rightarrow nt}^x \\ &+ v_{nt \leftarrow nm}^b v_{m't \rightarrow nt}^x, \end{aligned} \quad (38)$$

$$\begin{aligned} G_{nt}^{(1)}(\mathbb{E}[\xi_{nt}^u], \text{Var}[\xi_{nt}^u]) \\ = \log \int \mathcal{N}(u_{nt} | \mathbb{E}[\xi_{nt}^u], \text{Var}[\xi_{nt}^u]) \mu_{f_{u_{nt}} \leftarrow u_{nt}}(u_{nt}) du_{nt}, \end{aligned}$$

the superscript (i) , $i = 1, 2$ denotes the first layer and the second layer, respectively. For notational simplicity, the superscript is dropped in the following derivation. In the large system limits, $\mu_{x_{mt}}(x_{mt})$ is slightly different from $\mu_{x_{m't \rightarrow nt}}(x_{m't})$. We further use \hat{x}_{mt} to replace $\hat{x}_{m't \rightarrow nt}$. Besides, the items $v_{nt \leftarrow nm}^b v_{m't \rightarrow nt}^x \sim \mathcal{O}(\frac{1}{m})$ and $|\hat{h}_{nt \leftarrow nm}^b|^2 \sim \mathcal{O}(\frac{1}{m})$ are infinitesimal items that can be ignored [29]. Thus, we obtain

$$\begin{aligned} \log \mu_{x_{mt} \leftarrow f_{u_{nt}}}(x_{mt}) &\propto G_{nt}(\mathbb{E}[\xi_{nt}^u], \text{Var}[\xi_{nt}^u]) \\ &\propto G_{nt}(Z_{nt} + \hat{h}_{nm}^b(x_{mt} - \hat{x}_{mt}), V_{nt} + v_{nm}^b(|x_{mt}|^2 - |\hat{x}_{mt}|^2)). \end{aligned} \quad (39)$$

The Taylor series expansion is applied to $\log \mu_{x_{mt} \leftarrow f_{u_{nt}}}(x_{mt})$

$$\begin{aligned} &\log \mu_{x_{mt} \leftarrow f_{u_{nt}}}(x_{mt}) \\ &\propto G_{nt}(Z_{nt}, V_{nt}) + \hat{h}_{nm}^b(x_{mt} - \hat{x}_{mt}) G'_{nt}(Z_{nt}, V_{nt}) \\ &+ \frac{|\hat{h}_{nm}^b|^2 |x_{mt} - \hat{x}_{mt}|^2}{2} G''_{nt}(Z_{nt}, V_{nt}) + v_{nm}^b(|x_{mt}|^2 - |\hat{x}_{mt}|^2) \\ &\dot{G}_{nt}(Z_{nt}, V_{nt}) + \mathcal{O}(\frac{1}{m^{3/2}}) \\ &\propto x_{mt} \left(\hat{h}_{nm}^b G'_{nt}(Z_{nt}, V_{nt}) - |\hat{h}_{nm}^b|^2 \hat{x}_{mt} G''_{nt}(Z_{nt}, V_{nt}) \right) \\ &+ |x_{mt}|^2 \left(\frac{|\hat{h}_{nm}^b|^2}{2} G''_{nt}(Z_{nt}, V_{nt}) + v_{nm}^b \dot{G}_{nt}(Z_{nt}, V_{nt}) \right), \end{aligned} \quad (40)$$

where G'_{nt} and G''_{nt} are the first and second partial derivatives of G_{nt} w.r.t. the first argument, and \dot{G}_{nt} is the first derivative w.r.t. its second argument.

Thus, we obtain the first derivative of G_{nt}

$$\begin{aligned}\tilde{s}_{nt} &\triangleq G'_{nt} = \frac{\partial G_{nt}(Z_{nt}, V_{nt})}{\partial Z_{nt}} \\ &= \frac{\partial \log \int \mathcal{N}(u_{nt} | Z_{nt}, V_{nt}) \mu_{f_{u_{nt}} \leftarrow u_{nt}}(u_{nt}) du_{nt}}{\partial Z_{nt}} \\ &= \frac{\int \frac{(u_{nt} - Z_{nt})}{V_{nt}} \mathcal{N}(u_{nt} | Z_{nt}, V_{nt}) \mu_{f_{u_{nt}} \leftarrow u_{nt}}(u_{nt}) du_{nt}}{\int \mathcal{N}(u_{nt} | Z_{nt}, V_{nt}) \mu_{f_{u_{nt}} \leftarrow u_{nt}}(u_{nt}) du_{nt}} \\ &= \frac{\tilde{z}_{nt} - Z_{nt}}{V_{nt}},\end{aligned}\quad (41)$$

where $\frac{\mathcal{N}(u_{nt}|Z_{nt}, V_{nt}) \mu_{f_{u_{nt}} \leftarrow u_{nt}}(u_{nt})}{\int \mathcal{N}(u_{nt}|Z_{nt}, V_{nt}) \mu_{f_{u_{nt}} \leftarrow u_{nt}}(u_{nt}) du_{nt}} \sim \mathcal{N}(u_{nt}; \tilde{z}_{nt}, \tilde{v}_{nt})$.

The second partial derivation G''_{nt} is

$$\begin{aligned}v_{nt}^s &\triangleq -G''_{nt} = -\frac{\partial^2 G_{nt}(Z_{nt}, V_{nt})}{\partial Z_{nt}^2} \\ &= -\frac{\partial^2 \log \int \mathcal{N}(u_{nt} | Z_{nt}, V_{nt}) \mu_{f_{u_{nt}} \leftarrow u_{nt}}(u_{nt}) du_{nt}}{\partial Z_{nt}^2} \\ &= -\frac{\partial \int \frac{(u_{nt} - Z_{nt})}{V_{nt}} \mathcal{N}(u_{nt} | Z_{nt}, V_{nt}) \mu_{f_{u_{nt}} \leftarrow u_{nt}}(u_{nt}) du_{nt}}{\int \mathcal{N}(u_{nt} | Z_{nt}, V_{nt}) \mu_{f_{u_{nt}} \leftarrow u_{nt}}(u_{nt}) du_{nt}} / \partial Z_{nt} \\ &\propto -\frac{\tilde{v}_{nt} - V_{nt}}{V_{nt}^2}.\end{aligned}\quad (42)$$

The first partial derivation \dot{G}_{nt} is given

$$\begin{aligned}\dot{G}_{nt} &= \frac{\partial G_{nt}(Z_{nt}, V_{nt})}{\partial V_{nt}} \\ &= \frac{\int \left[\frac{(u_{nt} - Z_{nt})^2}{2V_{nt}^2} - \frac{1}{2V_{nt}} \right] \mathcal{N}(u_{nt} | Z_{nt}, V_{nt}) \mu_{f_{u_{nt}} \leftarrow u_{nt}}(u_{nt}) du_{nt}}{\int \mathcal{N}(u_{nt} | Z_{nt}, V_{nt}) \mu_{f_{u_{nt}} \leftarrow u_{nt}}(u_{nt}) du_{nt}} \\ &= \frac{\tilde{z}_{nt}^2 - 2\tilde{z}_{nt}Z_{nt} + Z_{nt}^2 + \tilde{v}_{nt} - V_{nt}}{2V_{nt}^2} = \frac{1}{2} [G'_{nt}{}^2 + G''_{nt}].\end{aligned}\quad (43)$$

The message can be further simplified as

$$\mu_{x_{mt} \leftarrow f_{u_{nt}}}(x_{mt}) \propto \int p\left(u_{nt} | x_{mt} h_{nm}^b + \sum_{m' \neq m} x_{m't} h_{nm'}^b\right) \quad (44)$$

$$\begin{aligned}&\mu_{f_{u_{nt}} \leftarrow u_{nt}} \prod_{m' \neq m} \mu_{x_{m't} \rightarrow f_{u_{nt}}} \prod_{m=1}^M \mu_{f_{u_{nt}} \leftarrow h_{nm}^b} du_{nt} dh_{nm}^b \\ &\sim \mathcal{N}\left(x_{mt} \mid \frac{\hat{h}_{nm}^b \tilde{s}_{nt} + \hat{x}_{mt} |\hat{h}_{nm}^b|^2 v_{nt}^s}{|\hat{h}_{nm}^b|^2 v_{nt}^s + v_{nm}^b v_{nt}^s - v_{nm}^b |\tilde{s}_{nt}|^2}, \frac{1}{|\hat{h}_{nm}^b|^2 v_{nt}^s + v_{nm}^b v_{nt}^s - v_{nm}^b |\tilde{s}_{nt}|^2}\right).\end{aligned}$$

Similarly, the message from $f_{u_{nt}}$ to h_{nm}^b is given by

$$\begin{aligned}&\mu_{f_{u_{nt}} \rightarrow h_{nm}^b}(h_{nm}^b) \\ &= f_{u_{nt}} \mu_{f_{u_{nt}} \leftarrow u_{nt}} \prod_{m' \neq m} \mu_{f_{u_{nt}} \leftarrow h_{nm'}^b} \prod_{m=1}^M \mu_{x_{mt} \rightarrow f_{u_{nt}}} \\ &\sim \mathcal{N}\left(h_{nm}^b \mid \frac{\hat{x}_{mt} \tilde{s}_{nt} + \hat{h}_{nm}^b |\hat{x}_{mt}|^2 v_{nt}^s}{|\hat{x}_{mt}|^2 v_{nt}^s + v_{mt}^x v_{nt}^s - v_{mt}^x |\tilde{s}_{nt}|^2}, \frac{1}{|\hat{x}_{mt}|^2 v_{nt}^s + v_{mt}^x v_{nt}^s - v_{mt}^x |\tilde{s}_{nt}|^2}\right).\end{aligned}\quad (45)$$

2) *The First Layer (Approximated Variable-to-Factor Messages)*: The message from x_{mt} to $f_{u_{nt}}$ in $(\ell + 1)$ -th iteration is given by

$$\mu_{x_{mt} \rightarrow f_{u_{nt}}}^{\ell+1}(x_{mt}) = p(x_{mt}) \prod_{n' \neq n} \mu_{x_{mt} \leftarrow f_{u_{n't}}}^{\ell}(x_{mt}), \quad (46)$$

where $p(x_{mt})$ is the (m, t) -th element of $p(\mathbf{X})$, and $p(\mathbf{X}) \sim \mathcal{N}(\mathbf{x}^0, \mathbf{v}_x^0)$ is a Gaussian mixture, thus we approximate it to be Gaussian with expectation propagation, which is crucial to achieve the low complexity implementation.

To deal with the discrete valued x_{mt} , the expectation propagation (EP) message $\tilde{p}(x_{mt})$ is used, where the EP message can be written as

$$\tilde{p}(x_{mt}) \propto \frac{\mu_{x_{mt}}(x_{mt})}{\prod_{n=1}^N \mu_{x_{mt} \leftarrow f_{u_{nt}}}}, \quad (47)$$

where $\mu_{x_{mt}}(x_{mt})$ is given in (52), and $\prod_{n=1}^N \mu_{x_{mt} \leftarrow f_{u_{nt}}}(x_{mt})$ is given in (53).

Thus, the Gaussian product item in message $\mu_{x_{mt} \rightarrow f_{u_{nt}}}(x_{mt})$ is

$$\prod_{n' \neq n} \mu_{x_{mt} \leftarrow f_{u_{n't}}}(x_{mt}) \propto \mathcal{N}\left(x_{mt} \mid R_{mt \setminus n}^x, \Sigma_{mt \setminus n}^x\right), \quad (48)$$

where

$$\begin{aligned}\Sigma_{mt \setminus n}^x &= \left(\sum_{n' \neq n} |\hat{h}_{n'm}^b|^2 v_{n't}^s + v_{n'm}^b v_{n't}^s - v_{n'm}^b |\tilde{s}_{n't}|^2 \right)^{-1}, \\ R_{mt \setminus n}^x &= \Sigma_{mt \setminus n}^x \left(\sum_{n' \neq n} \hat{h}_{n'm}^b \tilde{s}_{n't} + \hat{x}_{mt} |\hat{h}_{n'm}^b|^2 v_{n't}^s \right) \\ &= \hat{x}_{mt} \left(1 + \Sigma_{mt \setminus n}^x \sum_{n' \neq n} v_{n't}^b |\tilde{s}_{n't}|^2 - v_{n'm}^b v_{n't}^s \right) \\ &\quad + \Sigma_{mt \setminus n}^x \sum_{n' \neq n} \hat{h}_{n'm}^b \tilde{s}_{n't}.\end{aligned}\quad (49)$$

Thus,

$$\begin{aligned}\mu_{x_{mt} \rightarrow f_{u_{nt}}}^{\ell+1}(x_{mt}) &\sim p(x_{mt}) \mathcal{N}\left(x_{mt} \mid R_{mt \setminus n}^x, \Sigma_{mt \setminus n}^x\right) \\ &\sim \mathcal{N}\left(x_{mt} \rightarrow nt \mid \hat{x}_{mt \rightarrow nt}, v_{mt \rightarrow nt}^x\right),\end{aligned}\quad (50)$$

where

$$\begin{aligned}\hat{x}_{mt \rightarrow nt} &= \frac{1}{C} \int x_{mt} p(x_{mt}) \mathcal{N}\left(x_{mt} \mid R_{mt \setminus n}^x, \Sigma_{mt \setminus n}^x\right) dx_{mt} \\ &= g_{mt}\left(R_{mt \setminus n}^x, \Sigma_{mt \setminus n}^x\right), \\ v_{mt \rightarrow nt}^x &= \frac{1}{C} \int x_{mt}^2 p(x_{mt}) \mathcal{N}\left(x_{mt} \mid R_{mt \setminus n}^x, \Sigma_{mt \setminus n}^x\right) dx_{mt} \\ &\quad - \hat{x}_{mt \rightarrow nt}^2 = \Sigma_{mt \setminus n}^x g'_{mt}\left(R_{mt \setminus n}^x, \Sigma_{mt \setminus n}^x\right),\end{aligned}\quad (51)$$

and C is the normalization constant.

The belief of x_{mt} can be expressed as

$$\begin{aligned}\mu_{x_{mt}}(x_{mt}) &= \tilde{p}(x_{mt}) \prod_{n=1}^N \mu_{x_{mt} \leftarrow f_{u_{nt}}}(x_{mt}) \\ &\propto \tilde{p}(x_{mt}) \mathcal{N}\left(x_{mt} \mid R_{mt}^x, \Sigma_{mt}^x\right) \sim \mathcal{N}\left(x_{mt} \mid \hat{x}_{mt}, v_{mt}^x\right),\end{aligned}\quad (52)$$

where

$$\begin{aligned}\Sigma_{mt}^x &= \left(\sum_{n=1}^N |\hat{h}_{nm}^b|^2 v_{nt}^s + v_{nm}^b v_{nt}^s - v_{nm}^b |\tilde{s}_{nt}|^2 \right)^{-1}, \\ R_{mt}^x &= \Sigma_{mt}^x \left(\sum_{n=1}^N \hat{h}_{nm}^b \tilde{s}_{nt} + \hat{x}_{mt} |\hat{h}_{nm}^b|^2 v_{nt}^s \right) \\ &= \hat{x}_{mt} \left(1 - \Sigma_{mt}^x \sum_{n=1}^N v_{nm}^b v_{nt}^s \right) + \Sigma_{mt}^x \sum_{n=1}^N \hat{h}_{nm}^b \tilde{s}_{nt},\end{aligned}\quad (53)$$

and

$$\begin{aligned}\hat{x}_{mt} &= \frac{1}{C} \int x_{mt} p(x_{mt}) \mathcal{N}(x_{mt} | R_{mt}^x, \Sigma_{mt}^x) dx_{mt} \\ &= g_{mt}(R_{mt}^x, \Sigma_{mt}^x), \\ v_{mt}^x &= \frac{1}{C} \int x_{mt}^2 p(x_{mt}) \mathcal{N}(x_{mt} | R_{mt}^x, \Sigma_{mt}^x) dx_{mt} \\ &\quad - \hat{x}_{mt}^2 = \Sigma_{mt}^x g'_{mt}(R_{mt}^x, \Sigma_{mt}^x),\end{aligned}\quad (54)$$

where $g'_{mt}(R_{mt}^x, \Sigma_{mt}^x)$ is the partial derivation w.r.t. the first argument.

Similarly, the message from h_{nm}^b to $f_{u_{nt}}$ in the $(\ell + 1)$ -th iteration is given by

$$\mu_{f_{u_{nt}} \leftarrow h_{nm}^b}^{\ell+1}(h_{nm}^b) = p(h_{nm}^b) \prod_{t' \neq t} \mu_{f_{u_{nt'}} \rightarrow h_{nm}^b}^{\ell}(h_{nm}^b). \quad (55)$$

Thus, the Gaussian product item in message $\mu_{f_{u_{nt}} \leftarrow h_{nm}^b}^{\ell+1}(h_{nm}^b)$ is

$$\prod_{t' \neq t} \mu_{f_{u_{nt'}} \rightarrow h_{nm}^b}^{\ell}(h_{nm}^b) \propto \mathcal{N}(h_{nm}^b | R_{nm}^b \setminus t, \Sigma_{nm}^b \setminus t), \quad (56)$$

where

$$\begin{aligned}\Sigma_{nm}^b \setminus t &= \left(\sum_{t' \neq t} |\hat{x}_{mt'}|^2 v_{nt'}^s + v_{mt'}^x v_{nt'}^s - v_{mt'}^x |\tilde{s}_{nt'}|^2 \right)^{-1}, \\ R_{nm}^b \setminus t &= \Sigma_{nm}^b \setminus t \left(\sum_{t' \neq t} \hat{x}_{mt'} \tilde{s}_{nt'} + \hat{h}_{nm}^b |\hat{x}_{mt'}|^2 v_{nt'}^s \right).\end{aligned}\quad (57)$$

Thus,

$$\begin{aligned}\mu_{f_{u_{nt}} \leftarrow h_{nm}^b}^{\ell+1}(h_{nm}^b) &\sim p(h_{nm}^b) \mathcal{N}(h_{nm}^b | R_{nm}^b \setminus t, \Sigma_{nm}^b \setminus t) \\ &\sim \mathcal{N}(h_{nm}^b | \hat{h}_{nt \leftarrow nm}^b, v_{nt \leftarrow nm}^b),\end{aligned}\quad (58)$$

where

$$\begin{aligned}\hat{h}_{nt \leftarrow nm}^b &= \frac{1}{C} \int h_{nm}^b p(h_{nm}^b) \mathcal{N}(h_{nm}^b | R_{nm}^b \setminus t, \Sigma_{nm}^b \setminus t) dh_{nm}^b \\ &= g_{nm}(R_{nm}^b \setminus t, \Sigma_{nm}^b \setminus t), \\ v_{nt \leftarrow nm}^b &= \frac{1}{C} \int h_{nm}^b{}^2 p(h_{nm}^b) \mathcal{N}(h_{nm}^b | R_{nm}^b \setminus t, \Sigma_{nm}^b \setminus t) dh_{nm}^b \\ &\quad - \hat{h}_{nt \leftarrow nm}^b{}^2 = \Sigma_{nm}^b \setminus t g'_{nm}(R_{nm}^b \setminus t, \Sigma_{nm}^b \setminus t).\end{aligned}\quad (59)$$

The belief of h_{nm}^b

$$\begin{aligned}\mu_{h_{nm}^b}(h_{nm}^b) &= p(h_{nm}^b) \prod_{t=1}^T \mu_{f_{u_{nt}} \rightarrow h_{nm}^b}(h_{nm}^b) \\ &\sim p(h_{nm}^b) \mathcal{N}(h_{nm}^b | R_{nm}^b, \Sigma_{nm}^b) \sim \mathcal{N}(h_{nm}^b | \hat{h}_{nm}^b, v_{nm}^b),\end{aligned}\quad (60)$$

where

$$\begin{aligned}\Sigma_{nm}^b &= \left(\sum_{t=1}^T |\hat{x}_{mt}|^2 v_{nt}^s + v_{mt}^x v_{nt}^s - v_{mt}^x |\tilde{s}_{nt}|^2 \right)^{-1}, \\ R_{nm}^b &= \Sigma_{nm}^b \left(\sum_{t=1}^T \hat{x}_{mt} \tilde{s}_{nt} + \hat{h}_{nm}^b |\hat{x}_{mt}|^2 v_{nt}^s \right) \\ &= \hat{h}_{nm}^b \left(1 + \Sigma_{nm}^b \sum_{t=1}^T v_{mt}^x |\tilde{s}_{nt}|^2 - v_{mt}^x v_{nt}^s \right) \\ &\quad + \Sigma_{nm}^b \sum_{t=1}^T \hat{x}_{mt} \tilde{s}_{nt},\end{aligned}\quad (61)$$

and

$$\begin{aligned}\hat{h}_{nm}^b &= \frac{1}{C} \int h_{nm}^b p(h_{nm}^b) \mathcal{N}(h_{nm}^b | R_{nm}^b, \Sigma_{nm}^b) dh_{nm}^b \\ &= g_{nm}(R_{nm}^b, \Sigma_{nm}^b), \\ v_{nm}^b &= \frac{1}{C} \int h_{nm}^b{}^2 p(h_{nm}^b) \mathcal{N}(h_{nm}^b | R_{nm}^b, \Sigma_{nm}^b) dh_{nm}^b - \hat{h}_{nm}^b{}^2 \\ &= \Sigma_{nm}^b g'_{nm}(R_{nm}^b, \Sigma_{nm}^b),\end{aligned}\quad (62)$$

where $g'_{nm}(R_{nm}^b, \Sigma_{nm}^b)$ is the partial derivation w.r.t. first argument.

3) *The Second Layer (Approximated Factor-to-Variable Messages)*: Similarly, we define the approximate posterior distribution

$$\begin{aligned}\xi_{kt}^a &= p(a_{kt} | \mathbf{Y}) = u_{nt} \mu_{f_{a_{kt}} \leftarrow q_{kn}}(q_{kn}) + \\ &\quad \sum_{n' \neq n} \mu_{u_{n't} \rightarrow f_{a_{kt}}}(u_{n't}) \mu_{f_{a_{kt}} \leftarrow q_{kn'}}(q_{kn'}).\end{aligned}\quad (63)$$

The message from $f_{a_{kt}}$ to u_{nt} can be simplified as

$$\begin{aligned}\mu_{u_{nt} \leftarrow f_{a_{kt}}}(u_{nt}) &= \int p\left(a_{kt} | u_{nt} q_{kn} + \sum_{n' \neq n} u_{n't} q_{kn'}\right) \\ &\quad \mu_{f_{a_{kt}} \leftarrow a_{kt}} \prod_{n' \neq n} \mu_{u_{n't} \rightarrow f_{a_{kt}}} \prod_{n=1}^N \mu_{f_{a_{kt}} \leftarrow q_{kn}} da_{kt} dq_{kn} \\ &= \int p(a_{kt} | \xi_{nt}^a) \mu_{f_{a_{kt}} \leftarrow a_{kt}} da_{kt}.\end{aligned}\quad (64)$$

The mean and variance of the related random variable ξ_{kt}^a can be computed as

$$\begin{aligned}\mathbb{E}[\xi_{kt}^a] &= u_{nt} \hat{q}_{kt \leftarrow kn} + \sum_{n' \neq n} \hat{u}_{n't \rightarrow kt} \hat{q}_{kt \leftarrow kn'} \\ &= u_{nt} \hat{q}_{kt \leftarrow kn} + Z_{kt \setminus n},\end{aligned}\quad (65)$$

$$\begin{aligned}\text{Var}[\xi_{kt}^a] &= |u_{nt}|^2 v_{kt \leftarrow kn}^q + \sum_{n' \neq n} |\hat{u}_{n't \rightarrow kt}|^2 v_{kt \leftarrow kn}^q \\ &\quad + |\hat{q}_{kt \leftarrow kn'}|^2 v_{n't \rightarrow kt}^u + v_{kt \leftarrow kn'}^q v_{n't \rightarrow kt}^u \\ &= |u_{nt}|^2 v_{kt \leftarrow kn}^q + V_{kt \setminus n},\end{aligned}\quad (66)$$

where $\hat{q}_{kt \leftarrow kn}$ and $v_{kt \leftarrow kn}^q$ are the means and the variance of the message $\mu_{f_{a_{kt}} \leftarrow q_{kn}}$, respectively. In addition, $\hat{u}_{n't \rightarrow kt}$ and $v_{n't \rightarrow kt}^u$ are the means and the variance of the message $\mu_{u_{n't} \rightarrow f_{a_{kt}}}$, respectively.

We define

$$Z_{kt} = \sum_{n=1}^N \hat{u}_{nt \rightarrow kt} \hat{q}_{kt \leftarrow kn},$$

$$V_{kt} = \sum_{n=1}^N \left(|\hat{u}_{nt \rightarrow kt}|^2 v_{kt \leftarrow kn}^q + |\hat{q}_{kt \leftarrow kn}|^2 v_{nt \rightarrow kt}^u + v_{kt \leftarrow kn}^q v_{nt \rightarrow kt}^u \right). \quad (67)$$

Similarly, the logarithm of message $\mu_{u_{nt} \leftarrow f_{a_{kt}}}(u_{nt})$ is given by

$$\log \mu_{u_{nt} \leftarrow f_{a_{kt}}}(u_{nt}) \propto G_{kt}(\mathbb{E}[\xi_{kt}^a], \text{Var}[\xi_{kt}^a])$$

$$\propto G_{kt}(Z_{kt} + \hat{q}_{kn}(u_{nt} - \hat{u}_{nt}), V_{kt} + v_{kt \leftarrow kn}^q (|u_{nt}|^2 - |\hat{u}_{nt}|^2)). \quad (68)$$

The Taylor series expansion is applied to $\log \mu_{u_{nt} \leftarrow f_{a_{kt}}}(u_{nt})$

$$\log \mu_{u_{nt} \leftarrow f_{a_{kt}}}(u_{nt}) \propto G_{kt}(Z_{kt}, V_{kt}) + \hat{q}_{kn}(u_{nt} - \hat{u}_{nt})$$

$$G'_{kt}(Z_{kt}, V_{kt}) + \frac{|\hat{q}_{kn}|^2 |u_{nt} - \hat{u}_{nt}|^2}{2} G''_{kt}(Z_{kt}, V_{kt})$$

$$+ v_{kt \leftarrow kn}^q (|u_{nt}|^2 - |\hat{u}_{nt}|^2) \dot{G}_{kt}(Z_{kt}, V_{kt}) + \mathcal{O}\left(\frac{1}{m^{3/2}}\right), \quad (69)$$

where G'_{kt} and G''_{kt} are the first and second partial derivatives of G_{kt} w.r.t. the first argument, and \dot{G}_{kt} is the first derivative w.r.t. its second argument.

Thus, we obtain the first derivative of G_{nt}

$$\tilde{s}_{kt} \triangleq G'_{kt} = \frac{\partial G_{kt}(Z_{kt}, V_{kt})}{\partial Z_{kt}} = \frac{\tilde{z}_{kt} - Z_{kt}}{V_{kt}}, \quad (70)$$

where $\frac{\mathcal{N}(a_{kt}|Z_{kt}, V_{kt}) \mu_{f_{a_{kt}} \leftarrow a_{kt}}(a_{kt})}{\int \mathcal{N}(a_{kt}|Z_{kt}, V_{kt}) \mu_{f_{a_{kt}} \leftarrow a_{kt}}(a_{kt}) da_{kt}} \sim \mathcal{N}(a_{kt}; \tilde{z}_{kt}, \tilde{v}_{kt})$.

The second partial derivation G''_{kt} is

$$v_{nt}^s \triangleq G''_{kt} = \frac{\partial^2 G_{kt}(Z_{kt}, V_{kt})}{\partial Z_{kt}^2} \propto \frac{\tilde{v}_{kt} - V_{kt}}{V_{kt}^2}. \quad (71)$$

The first partial derivation \dot{G}_{kt} is

$$\dot{G}_{kt} = \frac{\partial G_{kt}(Z_{kt}, V_{kt})}{\partial V_{kt}} = \frac{1}{2} [G'_{kt}{}^2 + G''_{kt}]. \quad (72)$$

Thus, the message from $f_{v_{kt}}$ to u_{nt} can be simplified as

$$\mu_{u_{nt} \leftarrow f_{v_{kt}}}(u_{nt}) \sim \mathcal{N}\left(u_{nt} \mid \frac{\hat{q}_{kn} \tilde{s}_{kt} + \hat{u}_{nt} |\hat{q}_{kn}|^2 v_{kt}^s}{|\hat{q}_{kn}|^2 v_{kt}^s + v_{kn}^q v_{kt}^s - v_{kn}^q |\tilde{s}_{kt}|^2}, \quad (73)$$

$$\frac{1}{|\hat{q}_{kn}|^2 v_{kt}^s + v_{kn}^q v_{kt}^s - v_{kn}^q |\tilde{s}_{kt}|^2}\right).$$

Similarly, the message from $f_{a_{kt}}$ to q_{kn} is given by

$$\mu_{f_{a_{kt}} \rightarrow q_{kn}}(q_{kn})$$

$$= f_{a_{kt}} \mu_{f_{a_{kt}} \leftarrow a_{kt}} \prod_{n' \neq n} \mu_{f_{a_{kt}} \leftarrow q_{kn'}} \prod_{n=1}^N \mu_{u_{nt} \rightarrow f_{a_{kt}}}$$

$$\sim \mathcal{N}\left(q_{kn} \mid \frac{\hat{u}_{nt} \tilde{s}_{kt} + \hat{q}_{kn} |\hat{u}_{nt}|^2 v_{kt}^s}{|\hat{u}_{nt}|^2 v_{kt}^s + v_{nt}^u v_{kt}^s - v_{nt}^u |\tilde{s}_{nt}|^2}, \quad (74)$$

$$\frac{1}{|\hat{u}_{nt}|^2 v_{kt}^s + v_{nt}^u v_{kt}^s - v_{nt}^u |\tilde{s}_{nt}|^2}\right).$$

4) *The Second Layer (Approximated Variable-to-Factor Messages)*: The message from u_{nt} to $f_{a_{kt}}$ is given by

$$\mu_{u_{nt} \rightarrow f_{a_{kt}}}(u_{nt}) \sim \mu_{f_{u_{nt}} \rightarrow u_{nt}} \mathcal{N}(u_{nt} \mid R_{nt \setminus k}^u, \Sigma_{nt \setminus k}^u) \quad (75)$$

$$\sim \mathcal{N}(u_{nt \rightarrow kt} \mid \hat{u}_{nt \rightarrow kt}, v_{nt \rightarrow kt}^u),$$

where

$$\Sigma_{nt \setminus k}^u = \left(\sum_{t' \neq t}^T |\hat{q}_{kn}|^2 v_{kt'}^s + v_{kn}^q v_{kt'}^s - v_{kn}^q |\tilde{s}_{kt'}|^2 \right)^{-1}, \quad (76)$$

$$R_{nt \setminus k}^u = \Sigma_{nt \setminus k}^u \left(\sum_{t' \neq t}^T \hat{q}_{kn} \tilde{s}_{kt'} + \hat{u}_{nt'} |\hat{q}_{kn}|^2 v_{kt'}^s \right).$$

Thus, the belief of u_{nt} is

$$\mu_{u_{nt}}(u_{nt}) \sim \mu_{f_{u_{nt}} \rightarrow u_{nt}} \mathcal{N}(u_{nt} \mid R_{nt}^u, \Sigma_{nt}^u) \quad (77)$$

$$\sim \mathcal{N}(u_{nt} \mid \hat{u}_{nt}, v_{nt}^u).$$

Similarly,

$$\mu_{f_{a_{kt}} \leftarrow q_{kn}}(q_{kn}) \sim p(q_{kn}) \mathcal{N}(q_{kn} \mid R_{kn}^q, \Sigma_{kn \setminus t}^q) \quad (78)$$

$$\sim \mathcal{N}(q_{kn} \mid \hat{q}_{kt \leftarrow kn}, v_{kt \leftarrow kn}^q),$$

and the belief of q_{kn} is given by

$$\mu_{q_{kn}}(q_{kn})$$

$$p(q_{kn}) \prod_{t=1}^T \mu_{f_{a_{kt}} \rightarrow q_{kn}}(q_{kn}) \sim p(q_{kn}) \mathcal{N}(q_{kn} \mid R_{kn}^q, \Sigma_{kn}^q) \quad (79)$$

$$\sim \mathcal{N}(q_{kn} \mid \hat{q}_{kn}, v_{kn}^q).$$

5) *Simplifications of Intermediate Variables*: We further simplify

$$Z_{kt}^\ell = \sum_{n=1}^N \hat{u}_{nt \rightarrow kt}^\ell \hat{q}_{kt \leftarrow kn}^\ell = \sum_{n=1}^N \left(\hat{u}_{nt}^\ell - \hat{q}_{kn}^{\ell-1} \tilde{s}_{kt}^{\ell-1} v_{nt}^{u, \ell} \right)$$

$$\left(\hat{q}_{kn}^\ell - \hat{u}_{nt}^{\ell-1} \tilde{s}_{kt}^{\ell-1} v_{kn}^{q, \ell} \right)$$

$$\approx \sum_{n=1}^N \hat{u}_{nt}^\ell \hat{q}_{kn}^\ell - \tilde{s}_{kt}^{\ell-1} \sum_{n=1}^N \left(|\hat{q}_{kn}|^2 v_{nt}^{u, \ell} + |\hat{u}_{nt}|^2 v_{kn}^{q, \ell} \right) \quad (80)$$

$$= \bar{Z}_{kt}^\ell - \tilde{s}_{kt}^{\ell-1} \bar{V}_{kt}^\ell.$$

Moreover,

$$V_{kt}^\ell = \sum_{n=1}^N |\hat{u}_{nt \rightarrow kt}^\ell|^2 v_{kt \leftarrow kn}^{q, \ell} + |\hat{q}_{kt \leftarrow kn}^\ell|^2 v_{nt \rightarrow kt}^{u, \ell} + v_{kt \leftarrow kn}^{q, \ell} v_{nt \rightarrow kt}^{u, \ell}$$

$$= \sum_{n=1}^N |\hat{u}_{nt}^\ell - \hat{q}_{kn}^{\ell-1} \tilde{s}_{kt}^{\ell-1} v_{nt}^{u, \ell}|^2 v_{kn}^{q, \ell} + |\hat{q}_{kn}^\ell$$

$$- \hat{u}_{nt}^{\ell-1} \tilde{s}_{kt}^{\ell-1} v_{kn}^{q, \ell}|^2 v_{nt}^{u, \ell} + v_{kn}^{q, \ell} v_{nt}^{u, \ell}$$

$$\approx \bar{V}_{kt}^\ell + \sum_{n=1}^N v_{nt}^{u, \ell} v_{kn}^{q, \ell}. \quad (81)$$

Similarly,

$$Z_{nt}^\ell = \sum_{m=1}^M \hat{h}_{nt \leftarrow nm}^b \hat{x}_{mt \rightarrow nt} \approx \bar{Z}_{nt}^\ell - \tilde{s}_{nt}^{\ell-1} \bar{V}_{nt}^\ell, \quad (82)$$

$$V_{nt}^\ell \approx \bar{V}_{nt}^\ell + \sum_{m=1}^M v_{mt}^{x, \ell} v_{nm}^{b, \ell}.$$

We then simplify

$$\Sigma_{mt}^x = \left(\sum_{n=1}^N |\hat{h}_{nm}^b|^2 v_{nt}^s + v_{nt}^b v_{nt}^s - v_{nt}^b |\tilde{s}_{nt}|^2 \right)^{-1} \quad (83)$$

$$\approx \left(\sum_{n=1}^N |\hat{h}_{nm}^b|^2 v_{nt}^s \right)^{-1},$$

$$\Sigma_{nt}^u \approx \left(\sum_{k=1}^K |\hat{q}_{kn}|^2 v_{kt}^s \right)^{-1}. \quad (84)$$

6) *Message Between Different Layers*: The message from u_{nt} to $f_{u_{nt}}$ in ℓ -th iteration is given by

$$\mu_{f_{u_{nt}} \leftarrow u_{nt}}^\ell(u_{nt}) = \prod_{k=1}^K \mu_{u_{nt} \leftarrow f_{a_{kt}}}^\ell, \quad (85)$$

which is the product of large number of Gaussian distributions. By the Gaussian product property, we obtain

$$\mu_{f_{u_{nt}} \leftarrow u_{nt}}^\ell(u_{nt}) = \mathcal{N}(u_{nt} | R_{nt}, \Sigma_{nt}), \quad (86)$$

where

$$\Sigma_{nt} = \left(\sum_{k=1}^K \frac{1}{\Sigma_{kt}^u} \right)^{-1}, \quad R_{nt} = \Sigma_{nt} \left(\sum_{k=1}^K \frac{R_{kt}^u}{\Sigma_{kt}^u} \right), \quad (87)$$

with $\mu_{u_{nt} \leftarrow f_{a_{kt}}}(u_{nt}) \sim \mathcal{N}(u_{nt} | R_{kt}^u, \Sigma_{kt}^u)$.

Thus, $\zeta_{nt} = \frac{\mathcal{N}(u_{nt} | Z_{nt}, V_{nt}) \mu_{f_{u_{nt}} \leftarrow u_{nt}}^\ell(u_{nt})}{\int \mathcal{N}(u_{nt} | Z_{nt}, V_{nt}) \mu_{f_{u_{nt}} \leftarrow u_{nt}}^\ell(u_{nt}) du_{nt}} \sim \mathcal{N}(u_{nt}; \tilde{z}_{nt}, \tilde{v}_{nt})$ can be further updated as

$$\zeta_{nt} = \frac{\mathcal{N}(u_{nt} | Z_{nt}, V_{nt}) \mathcal{N}(u_{nt} | R_{nt}, \Sigma_{nt})}{\int \mathcal{N}(u_{nt} | Z_{nt}, V_{nt}) \mathcal{N}(u_{nt} | R_{nt}, \Sigma_{nt}) du_{nt}} \sim \mathcal{N}(u_{nt}; \tilde{z}_{nt}, \tilde{v}_{nt}), \quad (88)$$

where

$$\tilde{v}_{nt} = \left(\frac{1}{V_{nt}} + \frac{1}{\Sigma_{nt}} \right)^{-1}, \quad \tilde{z}_{nt} = \tilde{v}_{nt} \left(\frac{Z_{nt}}{V_{nt}} + \frac{R_{nt}}{\Sigma_{nt}} \right). \quad (89)$$

Similarly,

$$\zeta_{kt} = \frac{\mathcal{N}(a_{kt} | Z_{kt}, V_{kt}) \mathcal{N}(a_{kt} | R_{kt}, \Sigma_{kt})}{\int \mathcal{N}(a_{kt} | Z_{kt}, V_{kt}) \mathcal{N}(a_{kt} | R_{kt}, \Sigma_{kt}) da_{kt}} \sim \mathcal{N}(a_{kt}; \tilde{z}_{kt}, \tilde{v}_{kt}), \quad (90)$$

where

$$\tilde{v}_{kt} = \left(\frac{1}{V_{kt}} + \frac{1}{\Sigma_{kt}} \right)^{-1}, \quad \tilde{z}_{kt} = \tilde{v}_{kt} \left(\frac{Z_{kt}}{V_{kt}} + \frac{R_{kt}}{\Sigma_{kt}} \right). \quad (91)$$

REFERENCES

- [1] I. F. Akyildiz, C. Han, and S. Nie, "Combating the distance problem in the millimeter wave and terahertz frequency bands," *IEEE Commun. Mag.*, vol. 56, no. 6, pp. 102–108, June 2018.
- [2] S. Hu, F. Rusek, and O. Edfors, "Beyond massive MIMO: The potential of positioning with large intelligent surfaces," *IEEE Trans. Signal Process.*, vol. 66, no. 7, pp. 1761–1774, May 2018.
- [3] C. Huang, A. Zappone, G. C. Alexandropoulos, M. Debbah, and C. Yuen, "Reconfigurable intelligent surfaces for energy efficiency in wireless communication," *IEEE Trans. Wirel. Commun.*, vol. 18, no. 8, pp. 4157–4170, Aug. 2019.
- [4] M. Di Renzo, M. Debbah, D.-T. Phan-Huy, A. Zappone, M.-S. Alouini, C. Yuen, V. Sciancalepore, G. C. Alexandropoulos, J. Hoydis, H. Gacanin, J. de Rosny, A. Bounceur, G. Lerosey, and M. Fink, "Smart radio environments empowered by reconfigurable AI meta-surfaces: An idea whose time has come," *EURASIP J. Wireless Commun. Netw.*, vol. 2019, no. 1, pp. 1–20, May 2019.
- [5] Q. Wu and R. Zhang, "Towards smart and reconfigurable environment: Intelligent reflecting surface aided wireless network," *IEEE Commun. Mag.*, vol. 58, no. 1, Jan. 2020.
- [6] E. Calvanese Strinati et al., "Wireless environment as a service enabled by reconfigurable intelligent surfaces: The RISE-6G perspective," *Proc. Joint EuCNC & 6G Summit*, Porto, Portugal, 8–11 June 2021.
- [7] M. Di Renzo, A. Zappone, M. Debbah, M.-S. Alouini, C. Yuen, J. de Rosny, and S. Tretyakov, "Smart radio environments empowered by reconfigurable intelligent surfaces: How it works, state of research, and the road ahead," *IEEE J. Sel. Areas Commun.*, vol. 38, no. 11, pp. 2450–2525, Nov. 2020.
- [8] B. Yang, X. Cao, C. Huang, C. Yuen, L. Qian, and M. Di Renzo, "Intelligent spectrum learning for wireless networks with reconfigurable intelligent surfaces," *IEEE Trans. Veh. Tech.*, vol. 70, no. 4, pp. 3920–3925, Apr. 2021.
- [9] W. Tang, M. Z. Chen, X. Chen, J. Y. Dai, Y. Han, M. Di Renzo, Y. Zeng, S. Jin, Q. Cheng, and T. J. Cui, "Wireless communications with reconfigurable intelligent surface: Path loss modeling and experimental measurement," *IEEE Trans. Wirel. Commun.*, vol. 20, no. 1, pp. 421–439, Jan. 2021.
- [10] C. Huang, S. Hu, G. C. Alexandropoulos, A. Zappone, C. Yuen, R. Zhang, M. Di Renzo, and M. Debbah, "Holographic MIMO surfaces for 6G wireless networks: Opportunities, challenges, and trends," *IEEE Wirel. Commun.*, vol. 27, no. 5, pp. 118–125, Oct. 2020.
- [11] G. C. Alexandropoulos, N. Shlezinger, and P. del Hougne, "Reconfigurable intelligent surfaces for rich scattering wireless communications: Recent experiments, challenges, and opportunities," *IEEE Commun. Mag.*, vol. 59, no. 6, pp. 28–34, June 2021.
- [12] S. Hu, F. Rusek, and O. Edfors, "Beyond massive MIMO: The potential of data-transmission with large intelligent surfaces," *IEEE Trans. Signal Process.*, vol. 66, no. 10, pp. 2746–2758, May 2018.
- [13] C. Huang, R. Mo, and C. Yuen, "Reconfigurable intelligent surface assisted multiuser MISO systems exploiting deep reinforcement learning," *IEEE J. Sel. Areas Commun.*, vol. 38, no. 8, pp. 1839–1850, Aug. 2020.
- [14] Y. Han, W. Tang, S. Jin, C. Wen, and X. Ma, "Large intelligent surface-assisted wireless communication exploiting statistical CSI," *IEEE Trans. Veh. Technol.*, vol. 68, no. 8, pp. 8238–8242, Aug. 2019.
- [15] W. Yan, X. Yuan, and X. Kuai, "Passive beamforming and information transfer via large intelligent surface," *IEEE Wirel. Commun. Lett.*, vol. 9, no. 4, pp. 533–537, Apr. 2020.
- [16] T. Hou, Y. Liu, Z. Song, X. Sun, Y. Chen, and L. Hanzo, "Reconfigurable intelligent surface aided NOMA networks," *IEEE J. Sel. Area. Comm.*, vol. 38, no. 11, pp. 2575–2588, Nov. 2020.
- [17] Z. Peng, Z. Zhang, C. Pan, Li Li, and A. Lee S., "Multiuser full-duplex two-way communications via intelligent reflecting surface," *IEEE Trans. Sig. Process.*, vol. 69, pp. 837–851, Jan. 2021.
- [18] C. Pradhan, A. Li, L. Song, J. Li, B. Vucetic, and Y. Li, "Reconfigurable intelligent surface (RIS)-enhanced two-way OFDM communications," *IEEE Trans. Veh. Tech.*, vol. 69, no. 12, pp. 16270–16275, Dec. 2020.
- [19] A. Taha, M. Alrabeiah, and A. Alkhateeb, "Enabling large intelligent surfaces with compressive sensing and deep learning," *IEEE Access*, vol. 9, pp. 44304–44321, Mar. 2021.
- [20] C. Huang, Z. Yang, G. C. Alexandropoulos, K. Xiong, L. Wei, C. Yuen, Z. Zhang, and M. Debbah, "Multi-hop RIS-empowered terahertz communications: A DRL-based hybrid beamforming design," *IEEE J. Sel. Areas Commun.*, vol. 39, no. 6, pp. 1663–1677, June 2021.
- [21] L. Wei, C. Huang, G. C. Alexandropoulos, C. Yuen, Z. Zhang, and M. Debbah, "Channel estimation for RIS-empowered multi-user MISO wireless communications," *IEEE Trans. Commun.*, pp. 1–1, 2021.
- [22] C. You, B. Zheng, and R. Zhang, "Channel estimation and passive beamforming for intelligent reflecting surface: Discrete phase shift and progressive refinement," *IEEE J. Sel. Areas Commun.*, vol. 38, no. 11, pp. 2604–2620, Nov. 2020.
- [23] L. Wei, C. Huang, G. C. Alexandropoulos, Z. Yang, C. Yuen, and Z. Zhang, "Joint channel estimation and signal recovery in RIS-assisted multi-user MISO communications," in *2021 IEEE WCNC*, 2021, pp. 1–6.
- [24] J. T. Parker, P. Schniter, and V. Cevher, "Bilinear generalized approximate message passing—part i: Derivation," *IEEE Trans. Signal Process.*, vol. 62, no. 22, pp. 5839–5853, Nov. 2014.
- [25] X. Meng and J. Zhu, "A generalized sparse bayesian learning algorithm for 1-bit DOA estimation," *IEEE Commun. Lett.*, vol. 22, no. 7, pp. 1414–1417, July 2018.
- [26] S. Wu, L. Kuang, Z. Ni, D. Huang, Q. Guo, and J. Lu, "Message-passing receiver for joint channel estimation and decoding in 3D massive MIMO-OFDM systems," *IEEE Trans. Wirel. Commun.*, vol. 15, no. 12, pp. 8122–8138, Dec. 2016.
- [27] Y. Zhang, Z. Yuan, Q. Guo, Z. Wang, J. Xi, and Y. Li, "Bayesian receiver design for grant-free NOMA with message passing based structured signal estimation," *IEEE Trans. Veh. Technol.*, vol. 69, no. 8, pp. 8643–8656, Aug. 2020.
- [28] W. Yuan, N. Wu, Q. Guo, D. W. K. Ng, J. Yuan, and L. Hanzo, "Iterative joint channel estimation, user activity tracking, and data detection for FTN-NOMA systems supporting random access," *IEEE Trans. Commun.*, vol. 68, no. 5, pp. 2963–2977, May 2020.
- [29] Q. Zou, H. Zhang, and H. Yang, "Multi-layer bilinear generalized approximate message passing," *IEEE Trans. Sig. Process.*, vol. 69, pp. 4529–4543, Jul. 2021.
- [30] P. Schniter and S. Rangan, "Compressive phase retrieval via generalized approximate message passing," *IEEE Trans. Signal Process.*, vol. 63, no. 4, pp. 1043–1055, Feb. 2015.

- [31] X. Meng and J. Zhu, "Bilinear adaptive generalized vector approximate message passing," *IEEE Access*, vol. 7, pp. 4807–4815, 2019.
- [32] Z. Yuan, Q. Guo, and M. Luo, "Approximate message passing with unitary transformation for robust bilinear recovery," *IEEE Trans. Signal Process.*, vol. 69, pp. 617–630, 2021.
- [33] Q. Guo and J. Xi, "Approximate message passing with unitary transformation," *CoRR*, vol. *abs/1504.04799*, 2015. [Online]. Available: <http://arxiv.org/abs/1504.04799>.
- [34] Z. Shen, K. Xu, and X. Xia, "Beam-domain anti-jamming transmission for downlink massive MIMO systems: A stackelberg game perspective," *IEEE Trans. Information Forensics and Security*, vol. 16, pp. 2727–2742, 2021.
- [35] C.-K. Wen, S. Jin, K.-K. Wong, J.-C. Chen, and P. Ting, "Channel estimation for massive MIMO using gaussian-mixture bayesian learning," *IEEE Trans. Wirel. Commun.*, vol. 14, no. 3, pp. 1356–1368, Mar. 2015.
- [36] Da-Shan S., G. J. Foschini, M.J. Gans, and J.M. Kahn, "Fading correlation and its effect on the capacity of multielement antenna systems," *IEEE Trans. Commun.*, vol. 48, no. 3, pp. 502–513, Mar. 2000.
- [37] H. Xie, F. Gao, and S. Jin, "An overview of low-rank channel estimation for massive MIMO systems," *IEEE Access*, vol. 4, pp. 7313–7321, 2016.
- [38] S. Beygi, A. Elnakeeb, S. Choudhary, and U. Mitra, "Bilinear matrix factorization methods for time-varying narrowband channel estimation: Exploiting sparsity and rank," *IEEE Trans. Sig. Process.*, vol. 66, no. 22, pp. 6062–6075, Nov. 2018.
- [39] R. Zhang, H. Zhao, and J. Zhang, "Distributed compressed sensing aided sparse channel estimation in FDD massive MIMO system," *IEEE Access*, vol. 6, pp. 18383–18397, 2018.
- [40] K. Huang and N. D. Sidiropoulos, "Putting nonnegative matrix factorization to the test: a tutorial derivation of pertinent cramer—rao bounds and performance benchmarking," *IEEE Signal Process. Mag.*, vol. 31, no. 3, pp. 76–86, May 2014.
- [41] Y. Rong, M. R. A. Khandaker, and Y. Xiang, "Channel estimation of dual-hop MIMO relay system via parallel factor analysis," *IEEE Trans. Wirel. Commun.*, vol. 11, no. 6, pp. 2224–2233, June 2012.
- [42] Z. He and X. Yuan, "Cascaded channel estimation for large intelligent metasurface assisted massive MIMO," *IEEE Wirel. Commun. Lett.*, vol. 9, no. 2, pp. 210–214, Feb. 2020.